



HAL
open science

A new freshwater gobioid from the Lower Miocene of Turkey in a significantly amended total evidence phylogenetic framework

Moritz Dirnberger, Elena Bauer, Bettina Reichenbacher

► To cite this version:

Moritz Dirnberger, Elena Bauer, Bettina Reichenbacher. A new freshwater gobioid from the Lower Miocene of Turkey in a significantly amended total evidence phylogenetic framework. *Journal of Systematic Palaeontology*, 2024, 22 (1), pp.2340498. 10.1080/14772019.2024.2340498 . hal-04620463

HAL Id: hal-04620463

<https://hal.science/hal-04620463>

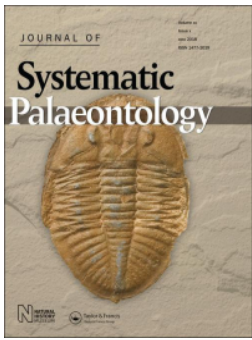
Submitted on 21 Jun 2024

HAL is a multi-disciplinary open access archive for the deposit and dissemination of scientific research documents, whether they are published or not. The documents may come from teaching and research institutions in France or abroad, or from public or private research centers.

L'archive ouverte pluridisciplinaire **HAL**, est destinée au dépôt et à la diffusion de documents scientifiques de niveau recherche, publiés ou non, émanant des établissements d'enseignement et de recherche français ou étrangers, des laboratoires publics ou privés.



Distributed under a Creative Commons Attribution 4.0 International License



A new freshwater gobioid from the Lower Miocene of Turkey in a significantly amended total evidence phylogenetic framework

Moritz Dirnberger, Elena Bauer & Bettina Reichenbacher

To cite this article: Moritz Dirnberger, Elena Bauer & Bettina Reichenbacher (2024) A new freshwater gobioid from the Lower Miocene of Turkey in a significantly amended total evidence phylogenetic framework, *Journal of Systematic Palaeontology*, 22:1, 2340498, DOI: [10.1080/14772019.2024.2340498](https://doi.org/10.1080/14772019.2024.2340498)

To link to this article: <https://doi.org/10.1080/14772019.2024.2340498>



© 2024 The Author(s). Published by Informa UK Limited, trading as Taylor & Francis Group.



[View supplementary material](#) 



Published online: 30 May 2024.



[Submit your article to this journal](#) 



[View related articles](#) 



[View Crossmark data](#) 



A new freshwater gobioid from the Lower Miocene of Turkey in a significantly amended total evidence phylogenetic framework

Moritz Dirnberger^{a,b} , Elena Bauer^a  and Bettina Reichenbacher^{a,c*} 

^aDepartment of Earth and Environmental Sciences, Ludwig-Maximilians-Universität München, Richard-Wagner Straße 10, 80333, Munich, Germany; ^bISEM, Univ Montpellier, CNRS, IRD, Montpellier, France; ^cGeoBio-Center Ludwig-Maximilians-Universität München, 80333, Munich, Germany

(Received 13 September 2023; accepted 25 March 2024)

The extant gobioid fishes form a highly diverse group comprised of eight families and over 2000 species. They pose many taxonomic and phylogenetic challenges, particularly when working with fossils. Here we introduce †*Simpsonigobius* gen. nov., a new freshwater gobioid of small size (≤ 34 mm) from the Lower Miocene of Turkey, and analyse its relationships using a total evidence phylogenetic framework from a previous study that we have significantly improved and expanded upon. †*Simpsonigobius* gen. nov. exhibits a unique combination of characters, including five branchiostegal rays, a palatine with a weakly 'T'-shaped head, an additional ray in the anal fin relative to the second dorsal fin, and rounded-to-quadrangular otoliths with a pronounced posterodorsal projection. Undated and tip-dated analyses in a total evidence Bayesian framework, utilizing our updated and expanded data set (48 extant in-group species, 10 fossil species, 48 morphological characters, data from five genes), indicate its relationship with the Oxudercidae, which is reinforced by our comparative morphological analysis. Our results reveal †*Simpsonigobius* gen. nov. as the oldest skeleton-based member of the Oxudercidae and the oldest freshwater species of the clade Gobiidae + Oxudercidae. The tip-dating analysis estimates divergence ages for Gobiidae (34.13 Ma) and Oxudercidae (34.83 Ma), which are in accordance with previous node-dating analyses. Additionally, based on our time-calibrated tree, we conduct the first reconstruction of ancestral habitat types employing stochastic character mapping and incorporating fossil taxa. The outcome reveals that the ancestor of the Gobioidae likely did not exclusively inhabit freshwater environments, challenging previous assumptions and emphasizing the importance of considering combined habitat types among early-splitting extant taxa. Our study represents the first simultaneous analysis of fossil and extant gobioid species, along with dating of the tree, and our data emphasize the ability of this approach to place gobioid fossils within a reliable chronological and phylogenetic context.

<http://zoobank.org/urn:lsid:zoobank.org:pub:5000841F-1836-43D8-BE75-4C090A478566>

Keywords: fossil Gobioidae; Oxudercidae; taxonomy; total evidence phylogeny

Introduction

The Gobioidae ('gobioids') is a suborder of the Teleostei, nested within the Percomorpha (Betancur-R et al., 2017). Gobioids encompass 325 genera with around 2330 species (Fricke et al., 2023) and are one of the most speciose clades among vertebrate suborders. These generally small and mainly benthic fishes are widely distributed, mostly in marine but also in brackish, freshwater and semi-terrestrial habitats (Patzner et al., 2011). In addition, they play an important ecological role by contributing to the recycling of nutrients and forming symbiotic relationships with other organisms, especially in coral reefs (Brandl et al., 2018; Patzner et al., 2011). Currently, gobioids are subdivided into the extinct family †Pirskeniidae Obrhelová, 1961 and eight extant families (Nelson et al., 2016; Reichenbacher et al., 2020), among which the Gobiidae + Oxudercidae represent the most derived clade (Fig. 1). The closest relative of the

Gobiidae + Oxudercidae is the Thalasseleotrididae, a small family which now consists of three genera and four species, all of which are restricted to the south-west Pacific (Goatley & Tornabene, 2022).

Molecular data strongly support the monophyly of extant gobioid families, and phylogenetic relationships between gobioid families are well established (Agorreta et al., 2013; Thacker, 2009; Thacker et al., 2015). However, only a few morphological synapomorphies are known for members of specific gobioid families, with synapomorphies remaining unknown for some families, such as the Odontobutidae or Oxudercidae (Hoese & Gill, 1993; Reichenbacher et al., 2018). This scarcity is due to various factors, including the tendency of derived gobioids to reduce bony structures, frequent occurrences of homoplasies and plesiomorphies, and the lack of comprehensive morphological studies, particularly with large data sets. Among those synapomorphies that define the Gobiidae + Oxudercidae are five branchiostegal

*Corresponding author. Email: b.reichenbacher@lrz.uni-muenchen.de

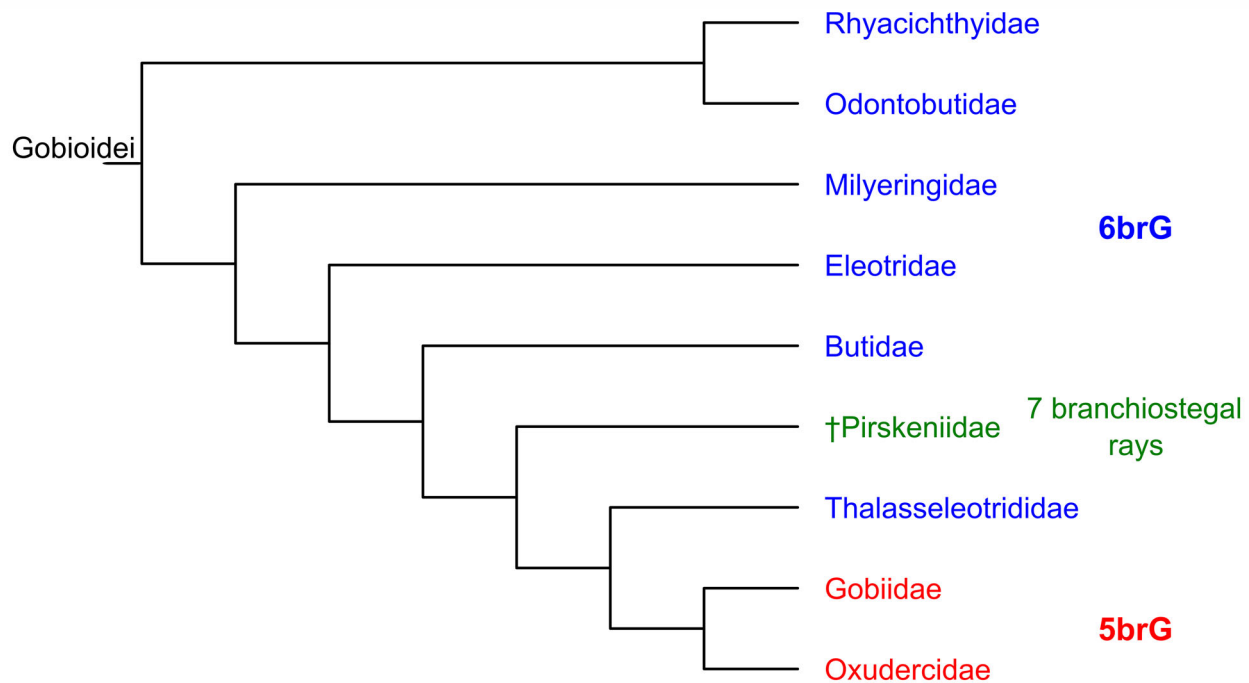


Figure 1. Phylogeny of the Gobioidei according to Betancur-R *et al.* (2017), Nelson *et al.* (2016), Reichenbacher *et al.* (2020) and Thacker (2009). **Abbreviations:** **5brG**, five branchiostegal ray gobioids; **6brG**, six branchiostegal ray gobioids.

rays – as opposed to six in all other extant families (A. C. Gill & Mooi, 2012; Hoese & Gill, 1993) and seven in the extinct family †Pirskeniidae (Fig. 1). The sole synapomorphy that unites the members of the Thalasseleotrididae is the presence of a long and broad membrane between the hyoid bar and ceratobranchial 1 (A. C. Gill & Mooi, 2012) – a character that is extremely unlikely to be preserved in a fossil.

The earliest known fossil gobioids date to the Eocene, with †*Carlomonnius quasigobius* Bannikov and Carnevale, 2016 from the lower Eocene of Monte Bolca (Northern Italy) and †*Paralates chapelcorneri* Gierl and Reichenbacher, 2017 from the upper Eocene of the Isle of Wight on the south coast of England representing the oldest records of skeleton-based species (Bannikov & Carnevale, 2016; Gierl & Reichenbacher, 2017). Several other extinct gobioid genera and species have been established on the basis of both skeletal and otolith material, especially from the Miocene (e.g. Lin *et al.*, 2017; Reichenbacher & Bannikov, 2022, 2023; Schwarzahns *et al.*, 2017; Schwarzahns, Brzobohatý, *et al.*, 2020), but also from Oligocene strata (Gierl *et al.*, 2013; Marramà *et al.*, 2022; Přikryl, 2014), as well as from Pliocene and Pleistocene sediments (Agiadi *et al.*, 2018, 2019, 2020; Schwarzahns, Agiadi, *et al.*, 2020). Notably, many of these fossil taxa are still lacking a phylogenetic context

because comparative morphology does not always enable their attribution at higher systematic (familial) levels. This situation arises not only because synapomorphies may be absent but also because a given fossil taxon may exhibit characters that are known to be typical for two (or more) of the extant families (see e.g. Bannikov & Carnevale, 2016; Gierl & Reichenbacher, 2015, 2017; Reichenbacher *et al.*, 2020). In such cases, a promising way forward is performing a total evidence phylogenetic analysis by combining molecular and morphological data from extant species with morphological data derived from fossil species (see López-Antoñanzas *et al.*, 2022). However, only one study has so far applied such a total evidence approach to gobioid fossils (Gierl *et al.*, 2022).

The present study focuses on a little-known fossil freshwater gobioid from the Lower Miocene at Karalar Köyü in western Turkey (Anatolia) (Fig. 2A, B). This fossil represents the oldest freshwater gobioid from the Miocene and is also the sole skeleton-based gobioid record from Anatolia. In the only previous study of this material (Rückert-Ülkümen, 2000), it was attributed to *Pomatoschistus* cf. *bleicheri* (Sauvage, 1883). This generic assignment, however, raises some doubts, as most extant species of the genus *Pomatoschistus* T. N. Gill, 1863 (family Oxudercidae) are marine (P. J. Miller, 1986; Tougaard *et al.*, 2014, 2021). Moreover, other fossil specimens that had been named

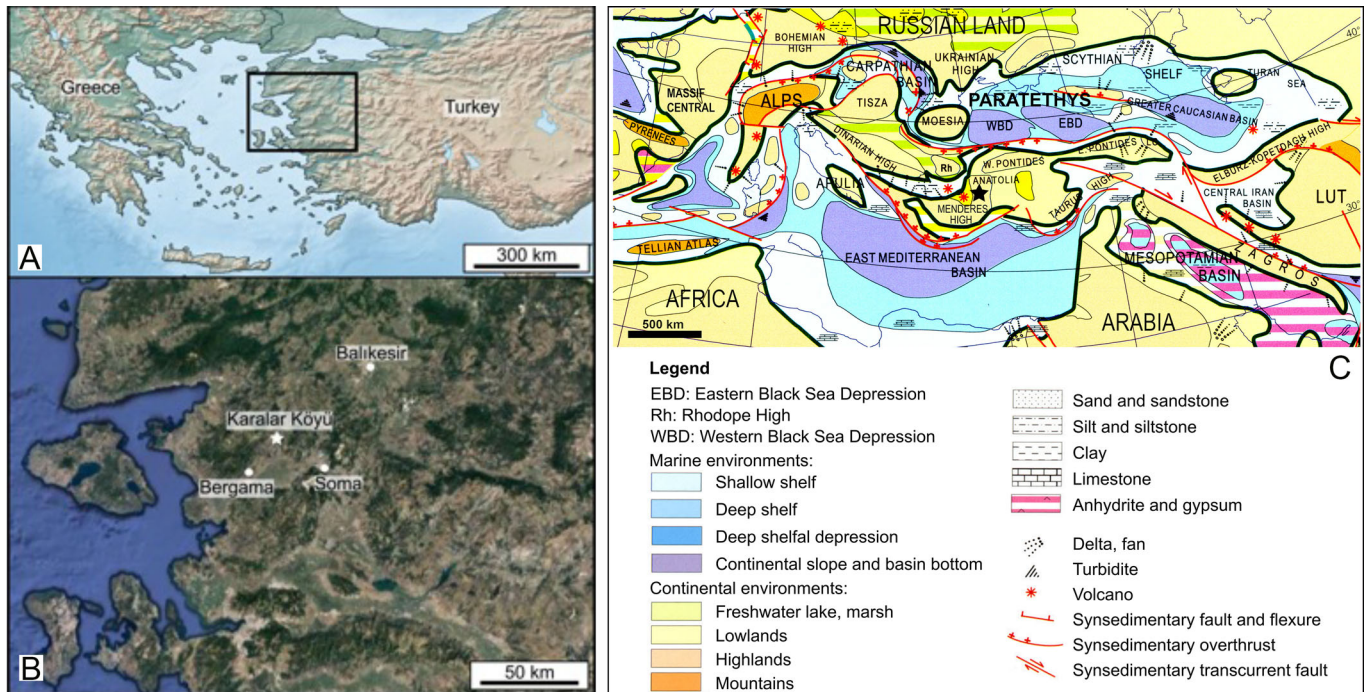


Figure 2. Geographic and palaeogeographic overview. **A**, geographic map of south-eastern Europe and Turkey (rectangle indicates map shown in B); **B**, map of Western Turkey showing location of the fossiliferous site Karalar Köyü (star); **C**, Early Miocene (20.5–19 Ma) palaeogeography of Central Europe and Western Asia and position of Karalar Köyü (star). Sources: A, B, <https://www.simplemappr.net/>; Imagery ©2022 TerraMetrics, Map data ©2022 Google; C, modified from Popov et al. (2004, map 4).

‘*Pomatoschistus bleicheri* (Sauvage, 1883)’ or ‘*P. cf. bleicheri* (Sauvage, 1883)’ in earlier studies are nowadays interpreted as members of the extinct gobioid genus †*Paralates* Sauvage, 1883, whose family relationships could not be resolved in previous work (Gierl et al., 2022; Gierl & Reichenbacher, 2017).

The primary objectives of our study are (i) to present a taxonomic revision of ‘*Pomatoschistus cf. bleicheri*’ from the Lower Miocene of Karalar Köyü and (ii) to analyse its phylogenetic relationships using both an undated and a tip-dated total evidence-based Bayesian framework. For the latter, we enhanced the morphological portion of the existing total evidence matrix (Gierl et al., 2022: 29 extant, 10 fossil gobioids, 48 characters) on the basis of a comprehensive literature review, and enlarged the taxon sample by adding morphological and molecular data for another 19 extant gobioid species. Our overall aim is to contribute to a better understanding of the evolutionary history of present-day Gobioidae by providing robust phylogenetic interpretations of their ancient members.

Geological setting

The fossil-bearing site Karalar Köyü is located in western Turkey, near the village of Karalar, about 27 km NNE of Bergama (Fig. 2A, B). It exposes an approximately 3 m

thick lacustrine succession, which consists of light grey to brownish limestones and shaley mudstones of the Zeytindağ Group (Kaya, 1981; Kaya et al., 2007; Rückert-Ülkümen, 2000). Karalar Köyü has been correlated with the Lower Miocene mammal zone MN3 (c. 17.2–19.5 Ma) based on fossil assemblages of rodents and lagomorphs from time-equivalent sediments in the same region (Göktaş & Ünay, 2000; Kaya et al., 2007). In terms of palaeogeography, Karalar Köyü was located on the huge lowland of present-day Turkey and western Asia that existed between the Eastern Paratethys Sea and the Eastern Mediterranean Basin in the Early Miocene (Popov et al., 2004) (Fig. 2C). Apart from ‘*Pomatoschistus cf. bleicheri*’, the cyprinid fish †*Palaeoleuciscus etilius* (Rückert-Ülkümen, 1960) and well-preserved plant remains have been recovered from the Lower Miocene sediments at Karalar Köyü (Gaudant, 1993; Rückert-Ülkümen, 2000).

Materials and methods

Fossil material

The fossil material from Karalar Köyü includes about 60 specimens, which are housed in the Bavarian State Collection for Palaeontology and Geology (SNSB-BSPG) under the numbers BSPG 1980X979–1025, 1980X1029, 1980X1030 (parts and counterparts of the

same specimens can have different BSPG numbers). When more than one specimen is preserved on a slab under the same collection number, a number in brackets was added for each specimen. The material includes more or less complete skeletons of 39 specimens, of which 18 were well enough preserved to be used for morphometric analyses. A further 16 specimens represent partially preserved skeletons, while the remaining five specimens consist of unidentifiable bone masses. Remains or imprints of otoliths are preserved *in situ* in 28 specimens (e.g. BSPG 1980X994, -1004, -1006), but all otoliths are heavily recrystallized. A complete list of the specimens is provided in [Supplemental material Table S1](#), sheet 1.

Meristic and osteological characters of the skeleton, together with otolith characters, were examined under a Leica MZ6 stereomicroscope equipped with a digital camera (type Gryphax Naos). Meristic counts include numbers of abdominal and caudal vertebrae (including the terminal centrum), number of spines in the first dorsal fin (D1), numbers of spines and rays in the second dorsal (D2), anal and pelvic fins, and the number of rays in the pectoral fin. Counting of the caudal-fin rays follows Fricke (1983). In fin formulae, numbers of spines are given in Roman numerals, and numbers of rays in Arabic numerals. Morphometric measurements of the skeletons follow Gut *et al.* (2020, fig. 1a) and include total length, standard length, distances from the snout to the beginning of D1, D2 and the anal fin, the distance from the posterior end of D2 to the caudal fin, the length of the caudal peduncle, the fin bases of D1, D2 and the anal fin, and the body depth at the anterior insertion of D1. In addition, the head length was measured from the snout to the cleithrum, and the maximum diameter of the eye was measured. All measurements were made using ImageJ (Schneider *et al.*, 2012) and standardized based on the standard length (or the head length in the case of the eye diameter). With the term ‘otolith’ we refer to the saccular otolith, and otolith terminology follows previous works (see Reichenbacher *et al.*, 2023).

Total evidence phylogenetic analysis

Enhancement of the previous character matrix. The total evidence matrix compiled by Gierl *et al.* (2022) included morphological and molecular data for 29 recent gobioid species (including at least two species per extant family) and 10 fossil gobioid species, with the apogonid *Sphaeramia nematoptera* Bleeker, 1856 as the outgroup. In the course of an extensive literature review, we noted that several of the 29 extant species studied exhibited more states per character than indicated in Gierl *et al.* (2022) (see [Supplemental material Table S2](#), sheet 1 for

details on literature), and we updated the matrix accordingly. If the literature data revealed that different character states each occurred frequently within a species (e.g. variable counts of vertebrae or fin rays), or if different character states were noted but their frequency was not stated, all described character states were implemented in the amended matrix. Only in cases where character states appeared to be ‘exceptional’ (i.e. present only in one or few specimens) were these states excluded. Moreover, additions and amendments were possible for two of the fossil species included in Gierl *et al.* (2022): (i) newly collected material of †*Paralates chapelcorneri* revealed several previously unknown characters of this species; and (ii) inspection of the syntypes and historical material of †*Eleogobius brevis* (Agassiz, 1839) revealed that some of its previously described character states need correction, e.g. presence of five rather than six branchiostegal rays. On the other hand, we discarded the fossil species †*Gobius francofurtanus* Koken, 1891 used in Gierl *et al.* (2022) from our taxon set, as the revision of this species is still pending and was not feasible in the context of our study. Details of all changes relative to the original matrix of Gierl *et al.* (2022) are listed in [Supplemental material Table S2](#), sheet 2. The amendments to the original matrix, with all changes indicated, are documented in [Supplemental material Table S3](#), Part A.

Enlargement of the taxon set used in the previous matrix. We added morphological and molecular data for 19 extant species and morphological data for the fossils from Karalar Köyü. The newly added extant species comprise one species each of the families Eleotridae and Thalasseleotrididae, three species of the family Gobiidae and 14 species of the family Oxudercidae ([Supplemental material Table S4](#)). The focus on the family Oxudercidae was based on the previous assignment of the specimens from Karalar Köyü to *Pomatoschistus*, which is a genus that belongs to this family.

For all species, except the thalasseleotridid species *Tempestichthys bettyae* Goatley & Tornabene, 2022, X-ray images were produced using a Faxitron Ultrafocus facility housed in the SNSB-ZSM or were downloaded from the Online Fish Collection Database maintained by the Smithsonian National Museum of Natural History (NMNH) in Washington, DC (see [Supplemental material Table S4](#) for details). For *T. bettyae*, micro-computed tomography (CT) scans from the study published by Goatley & Tornabene (2022) were available. Micro-CT scans could also be used (in addition to the X-ray images) for *Pomatoschistus minutus* (Pallas, 1770). New otolith data were available for five of the newly added species, i.e. *Acanthogobius*

flavimanus (Temminck & Schlegel, 1845), *Pseudogobius poecilosoma* (Bleeker, 1849), *Buenia affinis* Iljin, 1930, *Pomatoschistus minutus*, and *Sicydium crenilabrum* Harrison, 1993.

Based on the available X-ray and micro-CT resources, meristic and osteological characters of each extant species were examined. A comparison with literature data revealed that our results were congruent with character descriptions of the same species in previous publications (for references, see [Supplemental material Table S2](#)). However, for four species, meristic counts of the vertebrae and counts of fin elements are provided here for the first time, i.e. for *Gobiodon citrinus* (Rüppell, 1838), *Callogobius sclateri* (Steindachner, 1879), *Sicyopterus lagocephalus* (Pallas, 1770) and *Sicydium crenilabrum*. Character states of all extant species were coded (as far as possible) and implemented in the matrix. For the fossil species from Karalar Köyü, 23 morphological characters were recognized and inserted into the matrix. All new morphological data are compiled in [Supplemental material Table S3](#), Part B.

For 13 of the newly added extant species, molecular data, available from Agorreta et al. (2013), were incorporated into the matrix. For two of those species, one additional sequence could be downloaded from GenBank (Benson et al., 2013). The other six newly added species were not included in Agorreta et al. (2013), and their molecular data were downloaded from GenBank (Benson et al., 2013), wherever possible ([Supplemental material Table S4](#)). We included the same five genes used in Gierl et al. (2022): rDNA (12S rRNA, tRNA-Val, 16S rRNA), *cytb*, *rag1*, *zic1*, and *sreb2* (GPR85). We added the new molecular data to the alignments of the respective gene used in Gierl et al. (2022) and re-aligned them in AliView v. 1.28 (Larsson, 2014) with MUSCLE (Edgar, 2004). The alignments were then manually checked and trimmed where necessary. Afterwards they were concatenated into one matrix with 6349 base pairs using SeaView v. 5.0.5 (Gouy et al., 2010). Finally, a total evidence matrix was constructed by adding the morphological matrix (48 characters) to the molecular supermatrix in Mesquite v. 3.70 (Maddison & Maddison, 2021).

In total, our updated phylogenetic data set comprises morphological and molecular data for 48 extant gobioid species, compared to the 29 species included in the study of Gierl et al. (2022). It encompasses representatives from all three extant genera of the Thalasseleotrididae, each represented by one species; all five lineages of the Oxudercidae, each with two or more species; and 11 out of the 14 lineages of the Gobiidae, each with one or two species (the *Lophogobius*, *Kraemeria* and *Priolepis* lineages are the only ones not

included). Additionally, our data set incorporates the newly identified taxon from Karalar Köyü and, with the exception of †*G. francofurtanus*, all fossil species used in the previous matrix assembled by Gierl et al. (2022). All data matrices used are publicly available on figshare (<https://figshare.com/s/1c886af82e54c062531f>).

Undated phylogenetic analyses. Phylogenetic analyses were performed separately for the morphological, molecular and total evidence matrices based on Bayesian inference and, for comparison, also using implied-weights maximum parsimony. Bayesian inference analyses were carried out in MrBayes v. 3.2.7a (Ronquist et al., 2012), with parallel metropolis-coupled Markov chain Monte Carlo (MCMC) (Altekar et al., 2004; Geyer, 1991), using the Cyber-Infrastructure for Phylogenetic Research (CIPRES) Science Gateway v. 3.3 (M. A. Miller et al., 2010), for the morphological data under the Mkv+G model (Lewis, 2001; Yang, 1993) (following Gierl et al., 2022). For the molecular matrix, Agorreta et al. (2013) was followed, as the matrix used in our study was based on their work, and other recent studies follow them as well (Goatley & Tornabene, 2022). Accordingly, for best fitting substitution models, PartitionFinder2 (Guindon et al., 2010; Lanfear et al., 2017) was used with linked branch lengths and models restricted to the ones specific to MrBayes, based on the Bayesian information criterion (BIC) and the ‘greedy’ algorithm (Lanfear et al., 2012). The supermatrix was subdivided into four sub-data sets, with the *sreb2* and *zic1* genes combined. The GTR+I+G model (Churchill et al., 1992; Tavaré, 1986; Yang, 1993) was chosen for the rRNA+tRNA subset, HKY+I+G (Hasegawa et al., 1985) for the *cytb* and the combined *sreb2*+*zic1* subset, and SYM+I+G (Zharkikh, 1994) for the *rag1* subset. The analyses were performed following Gierl et al. (2022) with 2×4 MCMC chains for 5,000,000 generations, with sampling every 100th cycle and a burn-in of 25%. All Bayesian inference results were checked by examining the potential scale-reduction factor (PSRF) (Gelman & Rubin, 1992), the average standard deviation of split frequencies (Lakner et al., 2008) and the estimated sample size (ESS) as shown in MrBayes and in Tracer v. 1.7.2 (Rambaut et al., 2018). The resulting trees were summarized in a 50% majority-rule consensus tree with posterior probabilities (PP), which was visualized and rooted (in the case of non-clock analyses) in FigTree v. 1.4.4 (Rambaut, 2018).

Implied-weights maximum parsimony reconstructions were done in TNT v. 1.5 (Goloboff & Catalano, 2016) and followed Gierl et al. (2022) in using new technology searches (with sectorial search, ratchet, drift, and tree fusing; init. addseq = 100; find min.

Table 1. Geological ages of the fossils used for tip-dating. Age correlations of nannoplankton zones (NP), Palaeogene small mammal zones (MP) and Palaeogene chronostratigraphy follow Speijer *et al.* (2020), age correlation of Neogene mammal zones (MN) is according to Hilgen *et al.* (2012).

Fossil species	Geological age	Justification of geological age
† <i>Carlomonnius quasigobius</i> Bannikov & Carnevale, 2016	49.5–51 Ma	Shallow benthic biozonation 11 (Bannikov & Carnevale, 2016; Papazzoni <i>et al.</i> , 2014)
† <i>Paralates chapelcorneri</i> Gierl & Reichenbacher, 2017	35–36 Ma	Fishbourne Member, middle Priabonian (Bauer <i>et al.</i> , in review)
† <i>Paralates bleicheri</i> Sauvage, 1883	32–33 Ma	‘Marnes rouges à <i>Mytilus</i> ’ (Gaudant, 1979), corresponding to Middle Pechelbronn Formation (Martini & Reichenbacher, 2007), dated to nannoplankton zone NP 22 (Berger <i>et al.</i> , 2005)
† <i>Pirskenius diatomaceous</i> Obrhelová, 1961	28–31 Ma	K-Ar age of Bellon <i>et al.</i> (1998), see Reichenbacher <i>et al.</i> (2020)
† <i>Pirskenius radoni</i> Přikryl, 2014	27.82–33.9 Ma	Lower Oligocene, see Reichenbacher <i>et al.</i> (2020)
† <i>Lepidocottus aries</i> (Agassiz, 1839)	23.5–23.0 Ma	‘Calcaires et Marnes des stations d’essence’, dated to small mammal zone MP 30 (see Gierl <i>et al.</i> 2013)
† <i>Gobius jarosi</i> Přikryl & Reichenbacher, 2018	19.1–20.4 Ma	Nannoplankton data, see Reichenbacher <i>et al.</i> (2018)
†‘ <i>Eleogobius gaudanti</i> ’ Gierl & Reichenbacher, 2015	16.8–17.2 Ma	Kirchberg Formation (Gierl & Reichenbacher, 2015), dated by magnetostratigraphy and small mammal biostratigraphy (see Reichenbacher <i>et al.</i> 2013)
† <i>Eleogobius brevis</i> (Agassiz, 1839)	13 Ma	Age of type locality Öhningen according to Rasser <i>et al.</i> (2023)
Fossil from Karalar Köyü	17.2–19.5 Ma	Small mammal zone MN 3, see Geological setting (this study)

length = 10) and implied weighting with a concavity constant of $K = 12$ (Goloboff, 1993; Goloboff *et al.*, 2018). In cases of more than one most parsimonious tree, a 50% majority-rule consensus tree was calculated. Standard bootstrap (BS) resampling was done with 1000 replicates to calculate support values (new technology search; init. addseq = 10; find min. length = 5) (Felsenstein, 1985). Tree files and input files of all analyses are available on figshare (<https://figshare.com/s/1c886af82e54c062531f>).

Tip-dated phylogenetic analysis. For a time-calibrated, relaxed-clock Bayesian inference analysis, the uncorrelated independent gamma rate relaxed-clock model (Lepage *et al.*, 2007) was used. The dating was done by total evidence dating (tip-dating) (Ronquist, Klopfstein, *et al.*, 2012; Ronquist *et al.*, 2016). Following Zhang *et al.* (2016), a fossilized birth-death prior on the branch lengths and the ‘diversity’ sampling strategy were used (Höhna *et al.*, 2011; Stadler, 2010). The priors for the speciation, extinction and fossilization rates were retained as default (Exp(1.0), Beta(1.0,1.0), Beta(1.0,1.0)). The proportion of sampled species was calculated by dividing the number of extant gobioid taxa included in this study by the total number of extant gobioids (Fricke *et al.*, 2023) ($48/2330 = 0.0206$). For the prior used for the root age, an offset exponential distribution was used with a mean of 70 Ma (based on the split between Apogonoidei and Gobioidae ~ 70 Ma ago; Thacker, 2014) and a minimum of 52 Ma (oldest fossil gobioids, Bajpai & Kapur, 2004).

For tip-dating, geological ages of the included fossils were compiled based on existing biostratigraphic or magnetostratigraphic data for the respective fossil-bearing site (Table 1). To accommodate geological age uncertainties, uniform prior distributions were assigned to the fossil calibrations, except in the case of †*Eleogobius brevis* (see O’Reilly *et al.*, 2015). The prior of the variance increase parameter was retained as default (Exp(10)). An informative prior for the base rate of the clock was used following Ronquist *et al.* (2012): a strict-clock analysis was carried out to obtain the posterior distribution of the tree height. The median tree height was then divided by the tree age, resulting in an estimated rate of $0.454803/70 = 6.497 \times 10^{-3}$ substitutions per million base pairs per year. The prior for the base rate of the clock was set as a log-normal distribution, with the estimated rate as the mean and the exponent of the mean as the standard deviation (following Pyron, 2017): Lognorm(-5.036386 , $e^{0.454803}$). The clock model could not root the tree properly with *Sphaeramia nematoptera* as sister to all other taxa. Therefore, a topological constraint was added, forcing the included gobioids to form a monophyletic group (as in Simões *et al.*, 2018; Zhang *et al.*, 2016). The number of generations was increased to 10,000,000 for the MCMC, to ensure convergence between the runs. Bayesian inference results were checked as described above for the undated analyses by looking at the same mixing and convergence diagnostics.

Ancestral habitat reconstruction

To trace the evolutionary history of habitat on the phylogeny, the habitats of the extant taxa were initially sourced from FishBase (Froese & Pauly, 2023), encompassing freshwater, brackish, marine, or combinations of the three. Additionally, the habitat classifications for the fossil taxa were determined based on available literature sources. For our analysis, we utilized the relaxed clock maximum compatibility tree generated by MrBayes, which includes both the extant and the fossil taxa. However, †*Carlomonnus quasigobius* and the two species of †*Pirskenius* Obrhelová, 1961 were excluded due to uncertainties in their phylogenetic position, as revealed by the comparison of time-calibrated and non-calibrated trees. Stochastic character mapping involving 10,000 simulations was performed using v. 2.1.1 of the R package ‘phytools’ (Revell, 2024). Various models were examined using the ‘fitpolyMK’ function, encompassing scenarios with equal rates for all transitions, different rates for each transition, or distinct rates for gaining an additional habitat and losing one. These models were further combined with the option to order the states (freshwater ↔ brackish ↔ marine) or not, resulting in six distinct models. In all models, the combinations of states were considered to be intermediate between the respective states. The best model, determined by the Akaike information criterion, was the one with ordered states and equal rates, which was then selected for the stochastic character mapping analysis.

Institutional abbreviations

AMS: Australian Museum Sydney, Australia; **BMNH:** Museum of Natural History, London, UK (now NHMUK); **CAS-SU:** California Academy of Sciences, San Francisco, USA; **FMNH:** Field Museum of Natural History, Chicago, USA; **IRSNB:** Royal Belgian Institute of Natural Sciences, Brussels, Belgium; **NHMB:** Natural History Museum of Belgrade, Serbia; **NHMUK:** Natural History Museum, London, UK; **NMB:** ‘Neues Museum Biel’, Switzerland; **NMNZ:** Museum of New Zealand Te Papa Tongarewa, Wellington, New Zealand; **NMP:** National Museum Prague, Czech Republic; **NMW:** Natural History Museum Vienna, Austria (now NHMW); **NSMT:** National Science Museum, Department of Zoology, Tokyo, Japan; **SMF:** Senckenberg Research Institute and Natural History Museum, Frankfurt, Germany; **SMNS:** State Museum of Natural History, Stuttgart, Germany; **SNSB:** Bavarian Natural History Collections, Germany; **SNSB-BSPG:** Bavarian State Collection for Palaeontology and Geology, Munich, Germany; **SNSB-ZSM:** Bavarian State Collection of Zoology, Munich, Germany; **TUM:** Technical University of Munich, Germany; **UMG:**

Museum of Geology and Paleontology, University of Mining and Geology ‘St. Ivan Rilski’, Sofia, Bulgaria; **UMML:** University of Miami Marine Laboratory, USA; **USNM:** National Museum of Natural History, Washington, DC, USA; **UW:** University of Washington, Seattle, USA.

Systematic palaeontology

Taxonomic classification follows Nelson et al. (2016).

Series **Percomorpha** *sensu* Johnson and Patterson, 1993

Subseries **Gobiida** Nelson et al., 2016

Order **Gobiiformes** Günther, 1880

Genus †***Simpsonigobius*** gen. nov.

Type species. †*Simpsonigobius nerimanae* gen. et sp. nov.

Diagnosis. †*Simpsonigobius* gen. nov. is a small-sized gobioid fish up to 28.3 mm standard length (SL) with a moderately large head (head length 24–31% of SL), a mostly slender body (body depth 10–20% SL), a relatively long caudal peduncle measuring 23–32% of SL, and comparatively short bases of D2 and the anal fin (11–18% SL and 10–16% SL, respectively) (Fig. 3, Table 2). The new genus is further characterized by separated pelvic fins and the following combination of meristic characters: five branchiostegal rays, total number of vertebrae 26–27 (28?), with 10–11 abdominal, and 16–17 caudal vertebrae, D1 with six spines, D2 with spine and 9 rays, anal fin with spine and 10 rays, pectoral fin with 12–14 rays, and caudal fin with 13–14 branched and segmented rays. Characteristic osteological characters include a relatively slender premaxilla with either a weak or no postmaxillary process, a palatine with a relatively long shaft and weakly developed ‘T’-shaped head, and otoliths of rounded-to-quadrangular shape (L/H ratio 1.08) with a relatively large posterodorsal projection. Details of morphometric and meristic characters are presented in Table 2.

Derivation of name. The genus name honours Martin Simpson (Chale, Isle of Wight, UK), with whom a highly fruitful collaboration was established during the study of the rare species †*Paralates chapelcorneri*. This species plays an important role in the context of the new phylogenetic data matrix presented in this work.

Stratigraphic range. Lower Miocene, mammal zone MN3 (see ‘Geological setting’).

Table 2. Total and standard length (SL), morphometric measurements (in % SL, eye diameter in % HL) and meristic counts of †*Simpsonigobius nerimanae* gen. et sp. nov. For details of specimens, measurements and counts see Supplemental Table S1. **Abbreviations:** A, anal fin; D1, first dorsal fin; D2, second dorsal fin; SD, standard deviation.

	Holotype BSPG 1980X1030a + b	Paratypes (details in Suppl. Table S1)		ALL	
Total length (mm)	–	17.4–34.2		17.4–34.2	
Standard length (mm)	16.4	13.7–28.3		13.7–28.3	
Morphometric data	mm	% SL	mm (range)	% SL (range)	% SL (mean ± SD)
Snout to begin D1	–	–	5.4–9.1	34.6–42.2	38.7 (± 2.0)
Snout to begin D2	8.9	54.3	8.0–17.3	54.3–61.2	57.3 (± 1.7)
Snout to begin A	9.3	56.7	8.0–17.5	56.7–61.8	59.1 (± 1.4)
Length of caudal peduncle	4.6	28.0	4.2–7.8	23.0–32.5	28.1 (± 3.4)
Body depth	–	–	1.7–4.4	10.0–20.1	13.2 (± 2.3)
Base of D1	–	–	1.0–2.9	6.7–10.7	9.2 (± 1.4)
Base of D2	2.9	17.7	1.1–3.3	11.0–17.7	12.2 (± 2.9)
Base of A	2.6	15.9	1.4–4.4	9.5–15.9	13.1 (± 2.6)
Head length	4.0	24.1	3.7–8.3	24.1–31.3	27.8 (± 1.9)
Eye diameter (% HL)	–	–	1.0–1.6	18.7–34	26.4 (± 3.6)
Meristic data					Rückert-Ülkümen (2000)
Abdominal vertebrae	10		10–11 (mostly 10)		11
Caudal vertebrae	16		16–17		16
D1	VI		VI		VI
D2	I9		I9		I10
A	I10		I10		I10–11
Pelvic fin	I5		I5		I5
Pectoral fin	>10		c. 12–14		13
Branched caudal fin rays	–		13–14		12
Branchiostegal rays	–		5		7

Remarks and differential diagnosis. The distinct characteristics of †*Simpsonigobius* gen. nov., including its meristic traits and the presence of a palatine with a long shaft and a weakly ‘T’-shaped head, set it apart from all previously documented fossil gobioids. Although a palatine with a weakly ‘T’-shaped head has been recorded in †‘*Eleogobius*’ *gaudanti* (family incertae sedis) from the Lower Miocene of southern Germany, it is important to note that the genus †*Eleogobius* is not monophyletic and requires revision (Gierl *et al.*, 2022). Furthermore, a key difference lies in the branchiostegal rays, as †‘*E.*’ *gaudanti* shows six branchiostegal rays (Gierl & Reichenbacher, 2015), whereas †*Simpsonigobius* gen. nov. possesses five. Another significant difference is observed in the equality of rays in the D2 and anal fin in †‘*E.*’ *gaudanti*, whereas the anal fin exhibits one more ray than the D2 fin in †*S. nerimanae* gen. et sp. nov. Notably, this latter meristic character distinguishes †*Simpsonigobius* gen. nov. from all previously described fossil species from the Miocene of the Central and Eastern Paratethys, except for the species †*Hesperichthys reductus* Schwarzahns, Ahnelt, Carnevale and Japundžić, 2017. However, †*H. reductus* differs from †*S. nerimanae* gen. et sp. nov. in the total number of vertebrae (29 vs 26–27), more rays in the caudal fin (17 vs 13–14), and the

presence of rounded otoliths without any posterodorsal projection (see Schwarzahns *et al.* 2017).

Furthermore, as mentioned above, ‘*Pomatoschistus bleicheri* (Sauvage, 1883)’, to which Rückert-Ülkümen (2000) tentatively assigned the fossils from Karalar Köyü, is now †*Paralates bleicheri* Sauvage, 1883 (Gierl & Reichenbacher, 2017). However, there are distinct differences in meristic characters between †*Paralates* and †*Simpsonigobius* gen. nov. These include the numbers of abdominal vertebrae (10–11 in †*Simpsonigobius* gen. nov. vs 11–13 in †*Paralates*), caudal vertebrae (16–17 vs 17–19) and spines in the first dorsal fin (VI vs VII) – and it is obvious that the two genera are very different.

The only known extant genus that shares similarities with †*Simpsonigobius* gen. nov. in having a palatine with a weakly ‘T’-shaped head and similar abdominal and caudal vertebrae counts (10 + 16) is the monotypic genus *Tempestichthys* Goatley & Tornabene, 2022 of the family Thalasseleotrididae (see Goatley & Tornabene, 2022). However, *Tempestichthys* differs clearly from †*Simpsonigobius* gen. nov. in possessing six branchiostegal rays (vs five in †*Simpsonigobius* gen. nov.) and fewer rays both in the D2 (8 vs 9) and anal fin (7 vs 10) (see Goatley & Tornabene, 2022).

†*Simpsonigobius nerimanae* gen. et sp. nov.

(Figs 3–6, Table 2)

2000 *Pomatoschistus* cf. *bleicheri* (Sauvage, 1883); Rückert-Ülkümen: 157, pl. 2, fig. 4.

Diagnosis and differential diagnosis. As for genus.

Derivation of name. The species name honours Neriman Rückert-Ülkümen, who collected and described the fossil specimens from Karalar Köyü for the first time.

Material. Holotype: BSPG 1980X1030a, b, part and counterpart of complete skeleton, with otolith *in situ* (Fig. 3A). Paratypes: 27 moderately to well preserved skeletons, some with otoliths *in situ*: BSPG 1980X979, -981, -986/989(1), -988a + b, -989(2), -990a + b, -992a + b, -995(1)a + b, -995(2)a + b, -995(3)a + b, -997, -1000a + b, -1002(1), -1003a + b, -1004, -1006a + b, -1009(2)a + b, -1010(1)/1012(1), -1010(2)/1012(2), 1012(3), -1013(2), -1018, -1019a + b, -1020(1), -1020(2)/1025, -1022, 1024a + b. Further material: 27 specimens (see Supplemental material Table S1 for details).

Type locality and stratigraphy. Karalar Köyü, 27 km north of Bergama, western Turkey. Zeytindağ Group, upper Lower Miocene, small-mammal zone MN3, c. 17–20 Ma.

General description. Small gobioid (total lengths 17.4–34.2 mm) with slender body. The total number of vertebrae is 26–27 (10–11 + 16–17). D1 comprises six spines, the fin formula for D2 is I9 and for the anal fin I10. The palatine has a long shaft and relatively small ethmoid and maxillary processes (Figs 4A, 5A), resulting in a weakly developed ‘T’-shape of the palatine head; the endopterygoid is absent. There are five branchiostegal rays (Fig. 4C). Details of morphometric and meristic characters are provided in Table 2.

Neurocranium (Fig. 5A). The frontal bones show a narrow supraorbital and a much broader postorbital region (BSPG 1980X1010(1)). The parasphenoid is a long, straight, and slender bone that becomes progressively wider posteriorly towards the orbits (BSPG 1980X1016). The rounded-to-triangular vomer is visible anterior to the parasphenoid (Fig. 5A). Other bones of the neurocranium are unrecognizable.

Jaws (Fig. 5A–C). The anterior portion of the dentary is slender; posteriorly it appears to be made up of a larger posterodorsal and a posteroventral process (BSPG 1980X992a) (Fig. 5B). The angulo-articular is elongate-to-triangular in shape, but not optimally preserved. The jaw joint lies below the anteromedial portion of the orbit. The maxilla is a long, slender, relatively strongly curved bone. Its head displays a moderately long

process (*processus ascendens*) and a slightly concave incision for attachment to the articular process of the premaxillary (Fig. 5A). The premaxilla is a relatively slender bone. A needle-like ascending process is clearly visible (Fig. 5A, C), while the articular process is not well preserved but seems to be relatively short. A very weak postmaxillary process can be identified on the posterior third of the premaxilla in some specimens (Fig. 5C), while it seems to be absent in others. Both the dentary and the premaxilla bear small conical teeth, but their exact positions are not recognizable.

Suspensorium and opercular bones. The quadrate has a distinct articular condyle for articulation with the angulo-articular, and a robust and relatively long posterior process (Fig. 5A). The shape of the body of the quadrate is not clearly discernible, but seems to be triangular with a relatively broad dorsal margin (BSPG 1980X988b). The posterior portion of the symplectic is slightly widened, while the anterior part is stick-like and articulated with the posterior margin of the quadrate (Fig. 5A). Small remains of the metapterygoid seem to be present dorsal to the symplectic. The horizontal arm of the preopercle is ventrally adjoined to the posterior process of the quadrate; a faint hint of the lamina and the beginning of the curvature to the vertical arm are also visible. The opercle and subopercle are not well preserved: only a triangular outline of the opercle and the ventral margin of the subopercle are visible. Between the symplectic, the quadrate and the preopercle, the so-called *suspensorium fenestra* (or symplectic fenestra) is present.

The ectopterygoid is stick-like and widens slightly towards the quadrate; it connects to the anterior part of the quadrate, but its exact articulation with the latter cannot be clearly discerned (Fig. 5A). The endopterygoid is absent. The palatine is a straight, slender, dorsally slightly widened, relatively long bone; its ventral tip ends at approximately half the length of the ectopterygoid. The palatine head comprises a small maxillary and a small ethmoid process (clearly visible in BSPG 190X1019b), which together form a ‘T’-shape (Figs 4A, 5A).

Hyoid bar and branchiostegal rays (Fig. 4A, C). The ceratohyal is preserved in many specimens, but is usually displaced and rotated in a ventral direction (as shown in Fig. 4A). The anterior part of the ceratohyal is a relatively slender shaft, with a slight narrowing in its posterior half, while the posterior part of the ceratohyal becomes broader. The epihyal is not preserved. The branchiostegal rays were best preserved in laterally embedded specimens. As a result, the rays on one side overlap with those on the other, which complicated

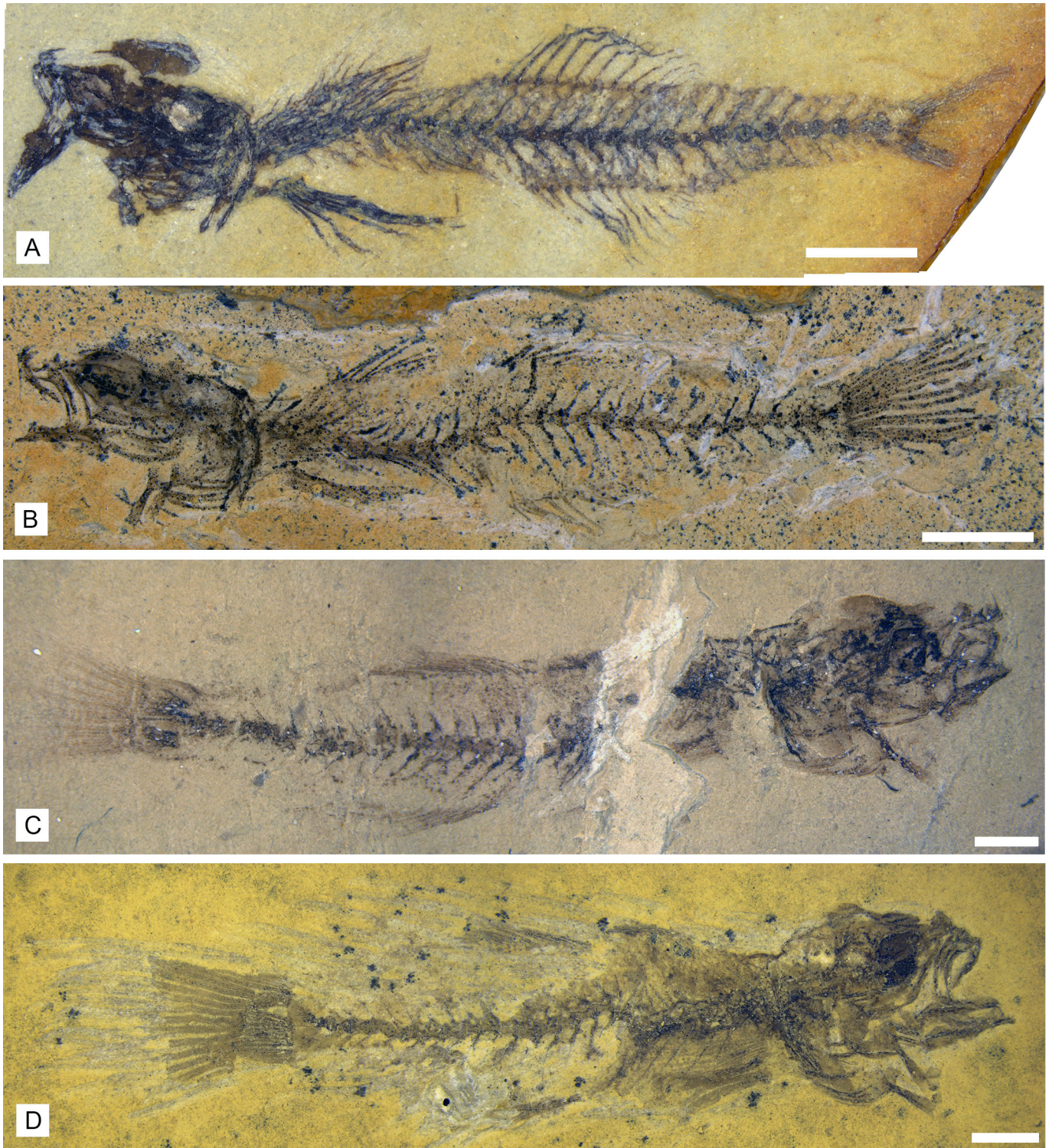


Figure 3. †*Simpsonigobius nerimanae* gen. et sp. nov. **A**, holotype, BSPG 1980X1030a; **B**, paratype, BSPG 1980X1013(2); **C**, paratype, BSPG 1980X1019a; **D**, paratype, BSPG 1980X992a. All scale bars = 2 mm.

efforts to determine their precise number. It seems likely that the count of seven branchiostegal rays mentioned by Rückert-Ülkümen (2000) resulted from this

overlapping of the right and left hyoid bars and their rays. However, in seven paratypes (BSPG 1980X988, -990a, -995, -1000, -1012(3), 1020(2), -1022), a number

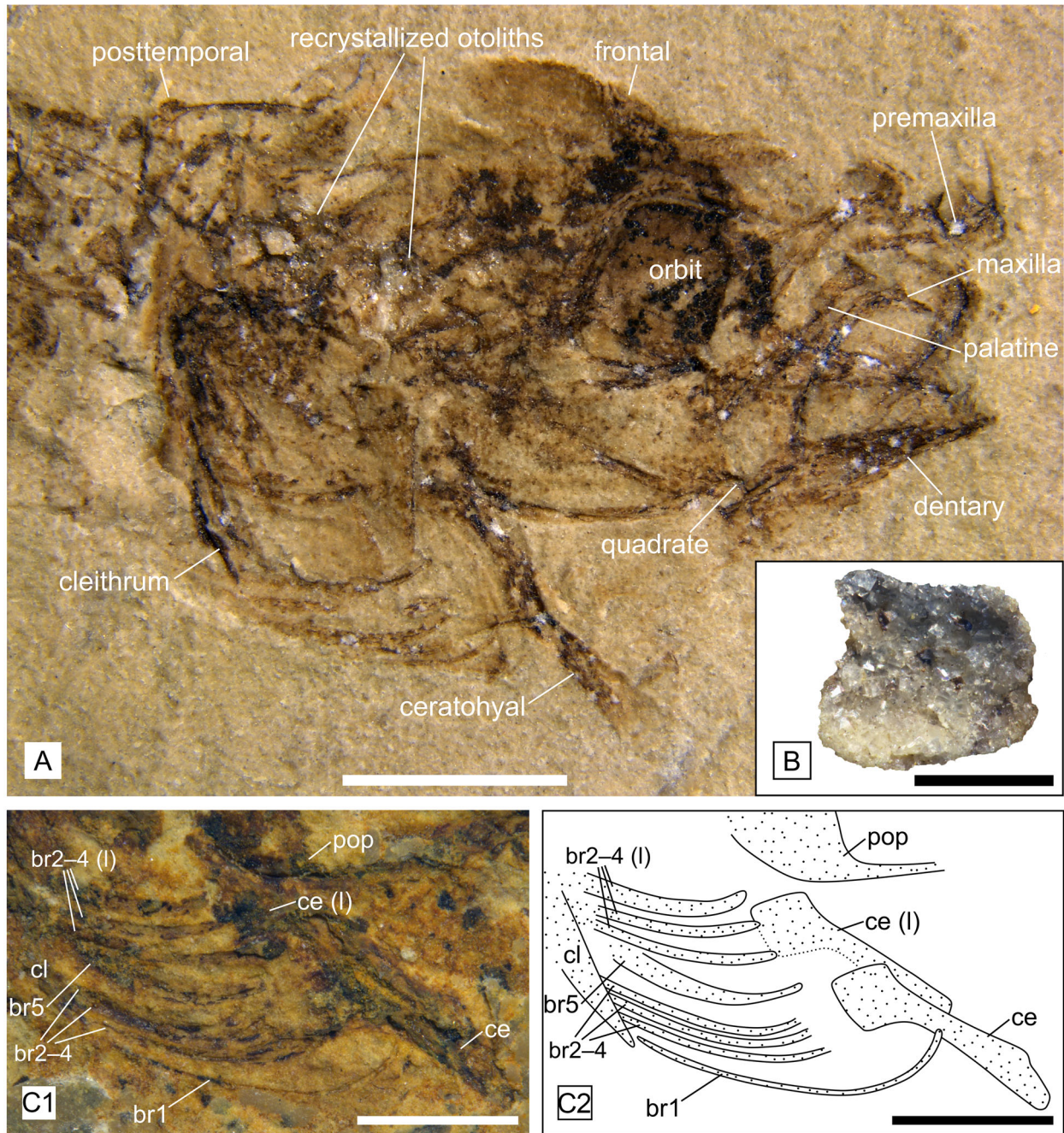


Figure 4. Head details of †*Simpsonigobius nerimanae* gen. et sp. nov. **A**, paratype BSPG 1980X1019a, head with strongly recrystallized otoliths *in situ*, scale bar = 2 mm; **B**, paratype BSPG 1980X1006b, otolith (recrystallized) preserved *in situ*, scale bar = 0.5 mm; **C**, paratype BSPG 1980X1020(2), photo (**C1**) and interpretative drawing (**C2**) of hyoid bar, bones from left side are indicated with '(l)', scale bar = 1 mm. **Abbreviations:** **br**, branchiostegal ray; **ce**, ceratohyal; **cl**, cleithrum; **pop**, preopercle.

of five branchiostegal rays is relatively clearly recognizable, as the two hyoid bars with their branchiostegal rays are slightly shifted relative to each other (Fig. 4C). The first branchiostegal ray is very thin and articulates at the narrower part of the anterior ceratohyal. After a gap, the broader branchiostegal rays 2–4 articulate close

to each other, with rays 2 and 3 being associated with the broadened posterior ceratohyal (BSPG 1980X981, -992a + b), while it cannot be recognized whether or not ray 4 articulates with the posterior ceratohyal or in the gap between it and the epihyal (Fig. 4C). The fifth and last branchiostegal is moderately expanded, and there is a

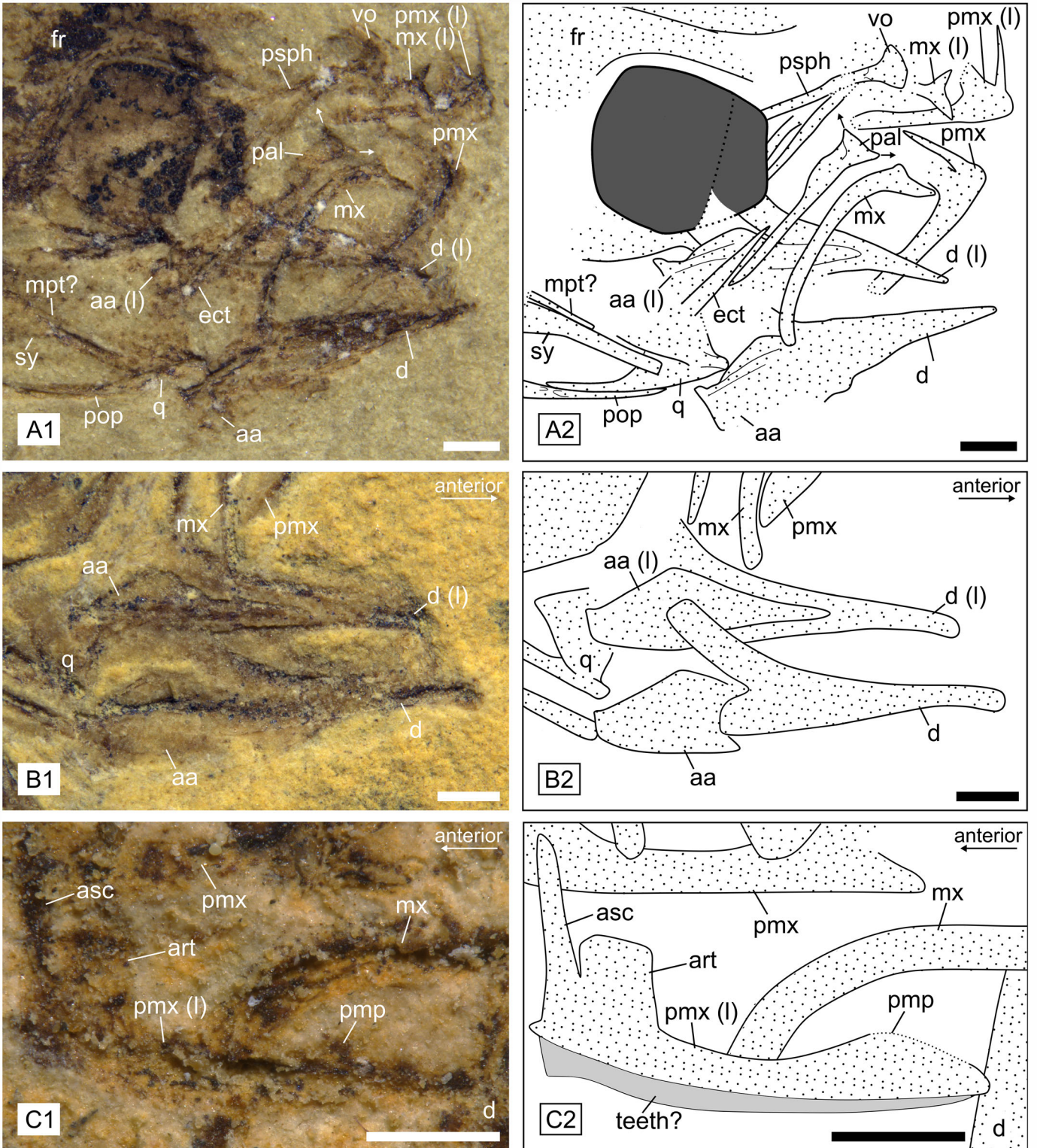


Figure 5. Details of skull and lower jaw of †*Simpsonigobius nerimanae* gen. et sp. nov. (photos and interpretative drawings). **A1, 2**, paratype BSPG 1980X1019 showing palatopterygoquadrate complex and weakly ‘T’-shaped palatine (pal, arrows indicate ethmoid and maxillary processes). **B1, 2**, paratype BSPG 1980X992a exhibiting left and right dentary (d) and angulo-articular (aa). **C1, 2**, paratype BSPG 1980X1022 displaying premaxilla with well-preserved ascending (asc) and articular (art) processes, partly preserved postmaxillary process (pmp) and remains of teeth. **Abbreviations:** aa, angulo-articular; art, articular process; asc, ascending process; d, dentary; ect, ectopterygoid; fr, frontal bones; mpt?, metapterygoid; mx, maxilla; pal, palatine; pmp, postmaxillary process; pmx, premaxilla; pop, preopercle; psph, parasphenoid; q, quadrate; sy, symplectic; vo, vomer. Left bones are indicated with ‘(l)’; all scale bars = 0.5 mm.

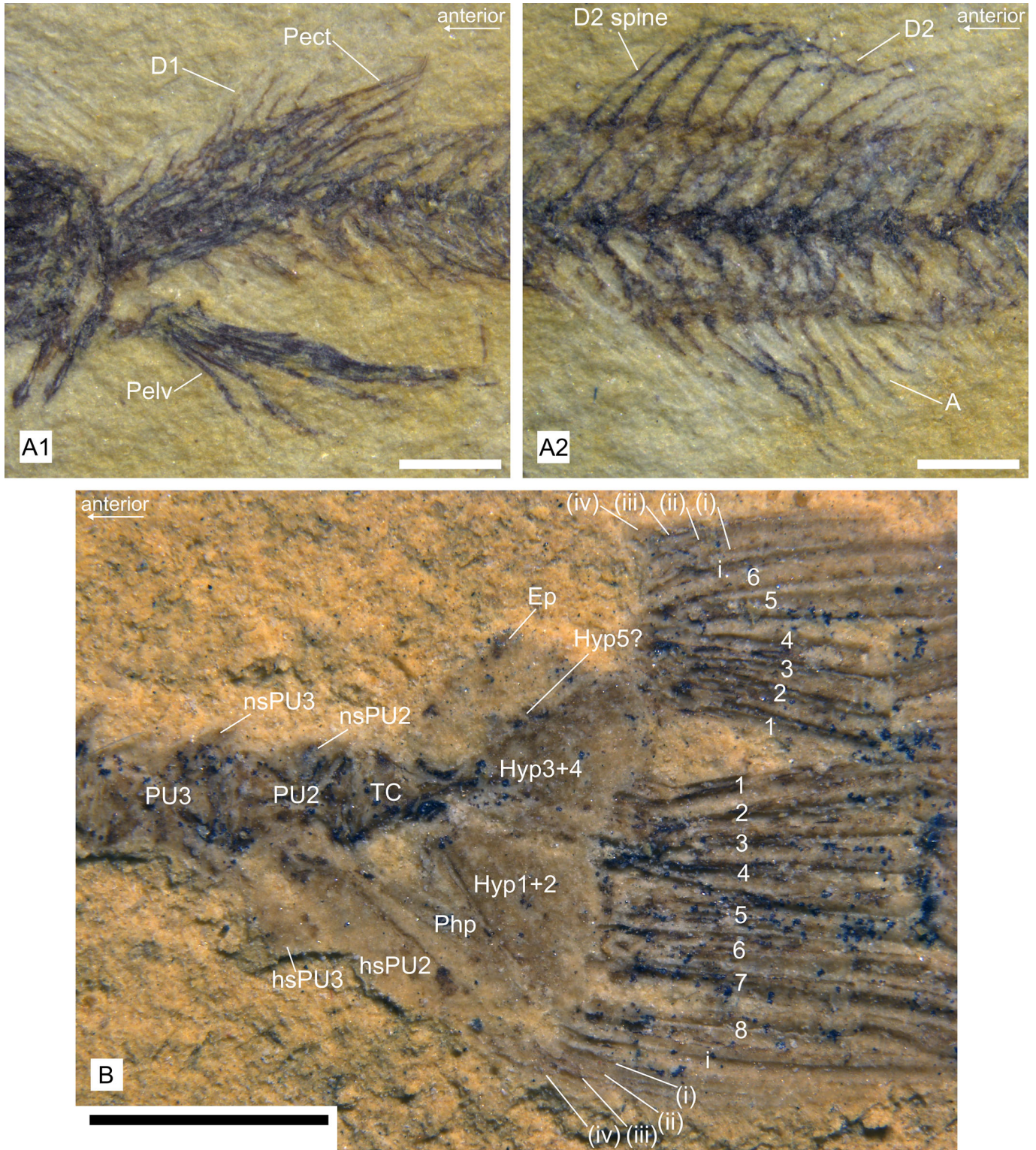


Figure 6. Details of fins of †*Simpsonigobius nerimanae* gen. et sp. nov. **A**, holotype BSPG 1980X1030a; **A1**, pelvic (Pelv) and pectoral (Pect) fins, first dorsal fin (D1, partly covered by Pect); **A2**, second dorsal fin (D2) and anal fin (A). **B**, paratype BSPG 1980X992b, caudal fin exposing six and eight branched rays in the upper and lower lobe, respectively, and caudal skeleton (note that neural spines of PU2 and PU3 and haemal spine of PU3 are only partly preserved). **Abbreviations:** **Ep**, epural; **hs**, haemal spine; **Hyp**, hypural plate; **ns**, neural spine; **Php**, parhypural; **PU**, preural vertebra; **TC**, terminal centrum. All scale bars = 1 mm.

clear gap between the fourth and fifth branchiostegal rays (BSPG 1980X981, -992a + b, -995(3)a + b). Although the epihyal is not preserved, this gap indicates that the fifth branchiostegal ray articulates at the epihyal.

Vertebral column. The specimens typically display 10 abdominal vertebrae, one specimen possesses 11 abdominal vertebrae (BSPG 1980X1018), and in several others the precise count as either 10 or 11 could not be determined (see [Supplemental material Table S1](#), sheet 2). The count of caudal vertebrae is usually 16, sometimes 17. Seven pairs of ribs are present, with no ribs attached to the first two and the last abdominal vertebrae. Epipleurals are connected to the ribs, but their exact number and shape is not discernible. The neural spines of all abdominal vertebrae are relatively long and equal in size, as are the neural spines of the caudal vertebrae, with the exceptions of the preural vertebra 3, which has a broadened neural spine, and preural vertebra 2, which has a short, triangular neural spine (BSPG 1980X1024a + b). Correspondingly, the haemal spines of the caudal vertebrae are equal in length and shape to the neural spines, except for preural vertebra 3 (which has a slightly broadened haemal spine) and preural vertebra 2 (with a clearly broadened haemal spine) ([Fig. 6B](#)).

Caudal skeleton and caudal fin ([Fig. 6B](#)). The caudal fin is somewhat fan-shaped, with a slightly rounded posterior margin. It consists of 13 to 14 segmented and branched rays, and one segmented but unbranched ray each dorsally and ventrally. There are at least three and up to five procurent rays each visible dorsally and ventrally (e.g. BSPG 1980X992b, -997), but they are often not well preserved and it is unclear whether additional procurent rays were present. Hypurals 1 and 2 are fused into one plate. Hypurals 3 and 4 are also fused to each other and to the terminal centrum. Remains of a small hypural 5 are located close to the plate of hypurals 3 + 4. There could be two narrow epurals in specimen 1980X992b, but due to poor preservation, it is not possible to state this with certainty. The parahypural can be discerned ventrally, close to the plate formed by hypurals 1 + 2 and next to the broadened haemal spine of the preural vertebra 2, but its shape could not be recognized.

Dorsal fins and anal fin ([Fig. 6A](#)). The first dorsal fin (D1) consists of six spines, the first two of which are located close to each other, while the last is positioned farther away from the others. The D1 pterygiophores are usually not well preserved, but the first pterygiophore appears to insert posterior to the neural spine of the third vertebra (BSPG 1980X988b). Judging from two specimens (BSPG 1980X988b, -1020(1)), the D1-ptyerygiophore formula can tentatively be determined as

3-21210. The second dorsal fin has a moderately long spine and nine rays; the anal fin bears a spine (its length is unclear) and 10 rays ([Fig. 6A2](#)).

Pectoral and pelvic fins ([Fig. 6A1](#)). In the pectoral girdle, the cleithrum is slightly curved and the post-temporal displays a long, slender anterodorsal process and a shorter posteroventral process (BSPG 1980X1019a, [Fig. 4A](#)); other details are not detectable. The pectoral fins each comprise 12–14 rays.

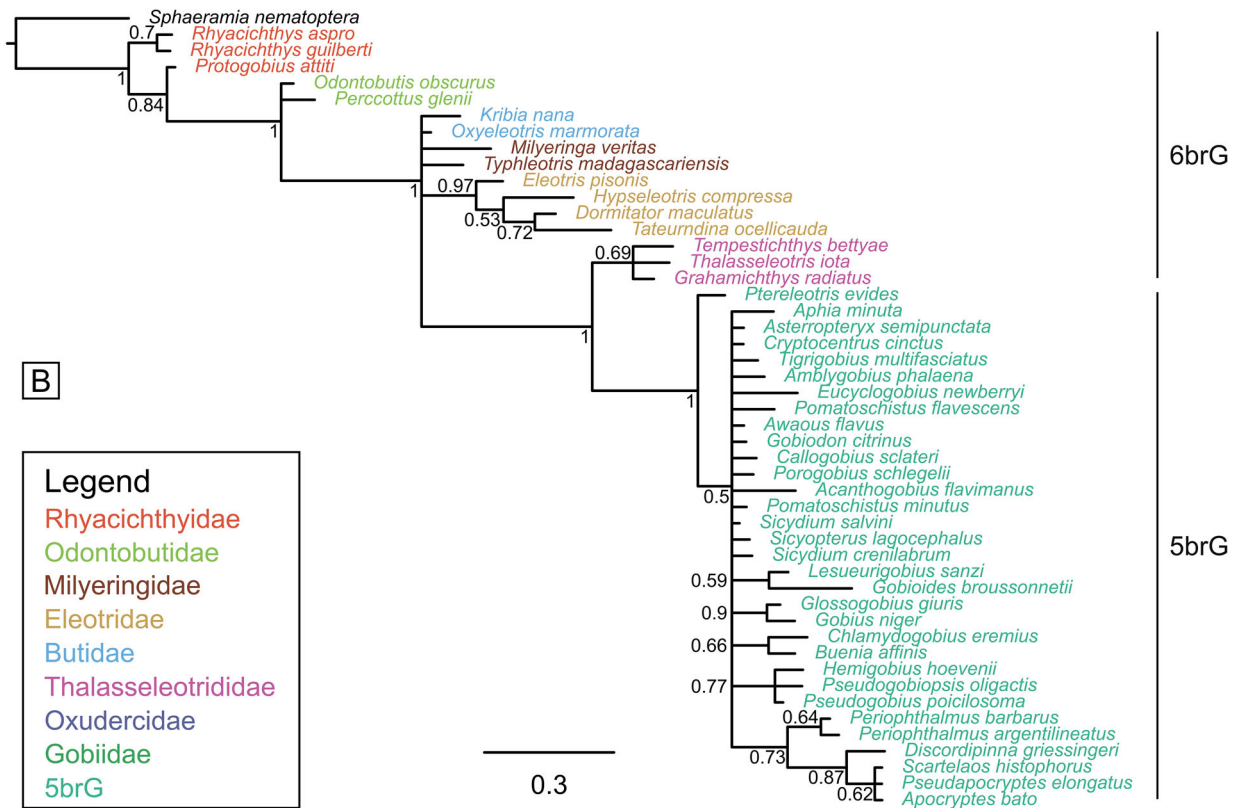
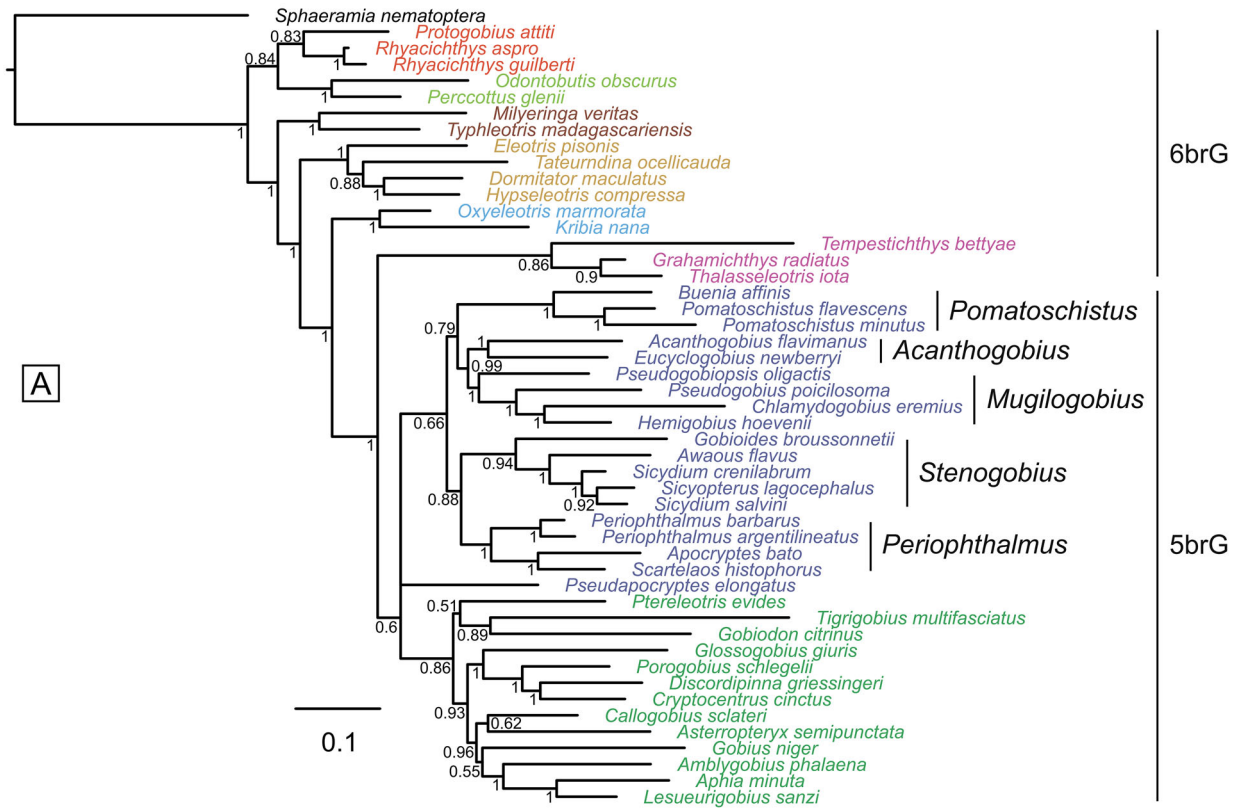
Parts of the pelvic bones are visible in BSPG 1980X1030a, but details are not preserved. The pelvic fins are longer than the pectoral fins (BSPG 1980X988b, 1030a) and located relatively far from each other (clearly visible in several specimens, see [Supplemental material Table S1](#), sheet 2), which suggests that the new species had separated pelvic fins. Each pelvic fin comprises one spine and five rays.

Otoliths. Otoliths are found *in situ* in 28 specimens ([Supplemental material Table S1](#)). Additionally, an otolith is found in the sediment directly next to the skeleton in specimen BSPG 1980X994. The otoliths are characterized by a rounded-to-quadrangular shape, a relatively large posterodorsal projection, a relatively small anteroventral projection, a bulging posteroventral margin and a rounded anterodorsal margin ([Fig. 4B](#)); the otolith length/height ratio is 1.08. All otoliths are heavily recrystallized, which precludes recognition of details of their medial surface.

Phylogenetic results based on the updated matrix

Tree of the extant species based on molecular data

Based on the molecular data for the 48 extant in-group species and the outgroup *Sphaeramia nematoptera*, Bayesian inference reconstruction (BI) resolved all gobioid families as monophyletic ([Fig. 7A](#)). The sole exception occurs in the Oxudercidae, as the oxudercid species *Pseudapocryptes elongatus* (Cuvier, 1816) forms a polytomy with the Gobiidae + Oxudercidae ([Fig. 7A](#)). Posterior probabilities are relatively high (PP \geq 0.83) for the families with six branchiostegal rays (6brG), but low (PP = 0.6) for Gobiidae + Oxudercidae (5brG). Among the five lineages of the Oxudercidae recognized by Agorreta *et al.* (2013), the *Periophthalmus* lineage is not recovered as monophyletic, owing to the unresolved position of *Ps. elongatus*. However, the other members of the *Periophthalmus* lineage are resolved as monophyletic – as are the representatives of the four remaining oxudercid lineages, each with high posterior



probabilities ($PP \geq 0.94$) (Fig. 7A). Among the Gobiidae, only one species per lineage was used in most cases, but the *Cryptocentrus* and *Aphia* lineages (each represented by two species) are resolved as monophyletic ($PP = 1$) (Fig. 7A). Moreover, phylogenetic relationships between families are congruent with previously published phylogenies (e.g. Agorreta *et al.*, 2013; Goatley & Tornabene, 2022; Thacker *et al.*, 2015). The relationships between the five oxudercid lineages are also congruent with previous studies (e.g. McCraney *et al.*, 2020).

In the maximum parsimony (MP) analysis, a single most parsimonious tree was reconstructed (Supplemental material Fig. S1A). All families, including the Oxudercidae, are recovered as monophyletic. Family relationships mostly resemble those revealed by the BI analysis. Among the Oxudercidae, four lineages are resolved as monophyletic, whereas the *Stenogobius* lineage (which includes *Ps. elongatus*) is not, owing to the ambiguous position of the latter as a member of the *Periophthalmus* lineage.

Tree of the extant species based on morphological data

The BI analysis based on the morphological data for the 48 extant in-group species and *Sphaeramia nematoptera* as outgroup only resolves the families Thalasseleotrididae ($PP = 0.69$) and Eleotridae ($PP = 0.97$) as monophyletic (Fig. 7B). Gobiidae + Oxudercidae (5brG) are resolved with maximal support ($PP = 1$) and the Thalasseleotrididae are positioned as sister to them. However, neither the relationships of the Eleotridae nor those within the 5brG clade are resolved. Even the well-established sister-group relationship of Rhyacichthyidae + Odontobutidae to the remaining families is not confirmed. In the MP analysis, the topology of the 50% majority-rule consensus tree is mostly similar to that of the BI analysis (Supplemental material Fig. S1B). Strong support is also observed for the 5brG clade (Bootstrap support [BS] = 90%), but notably diminishes for Eleotridae (BS = 58%). Conversely, support increases for Thalasseleotrididae (BS = 84%) (Supplemental material Fig. S1B).

Tree of the extant species based on the total evidence data set

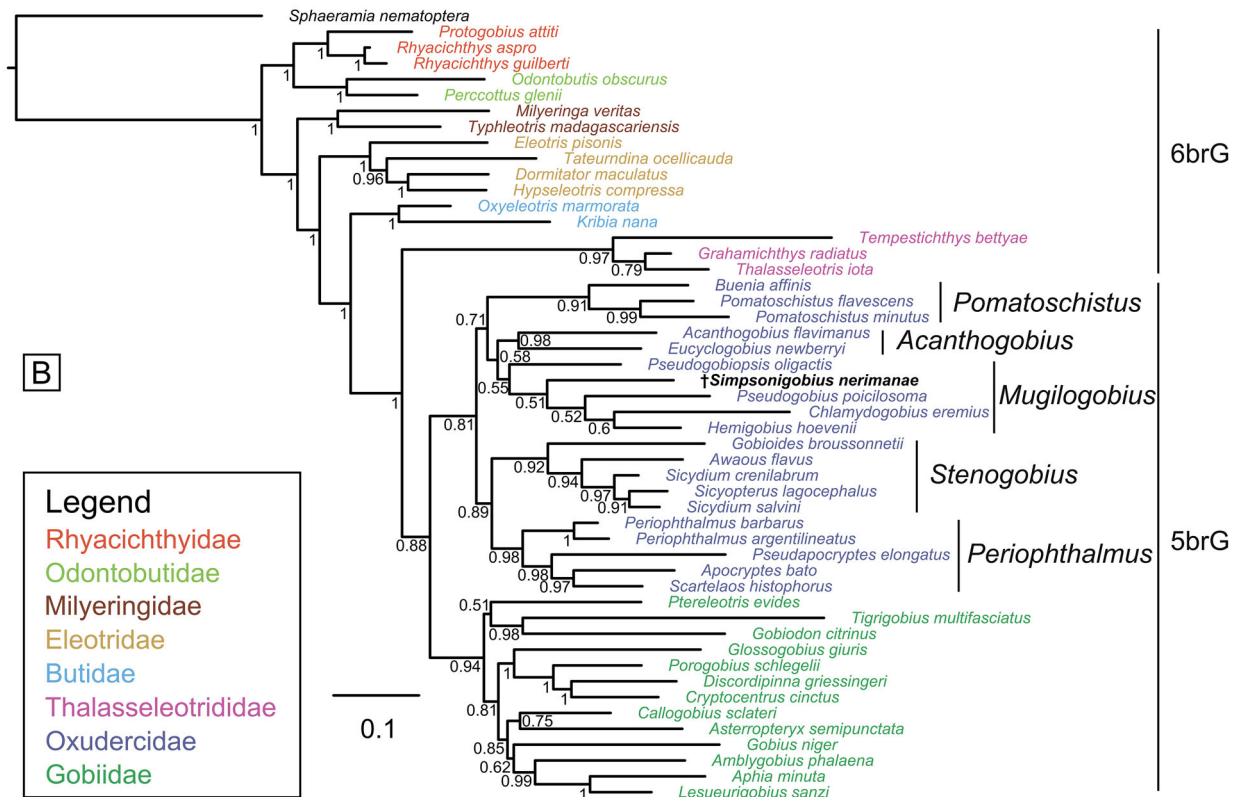
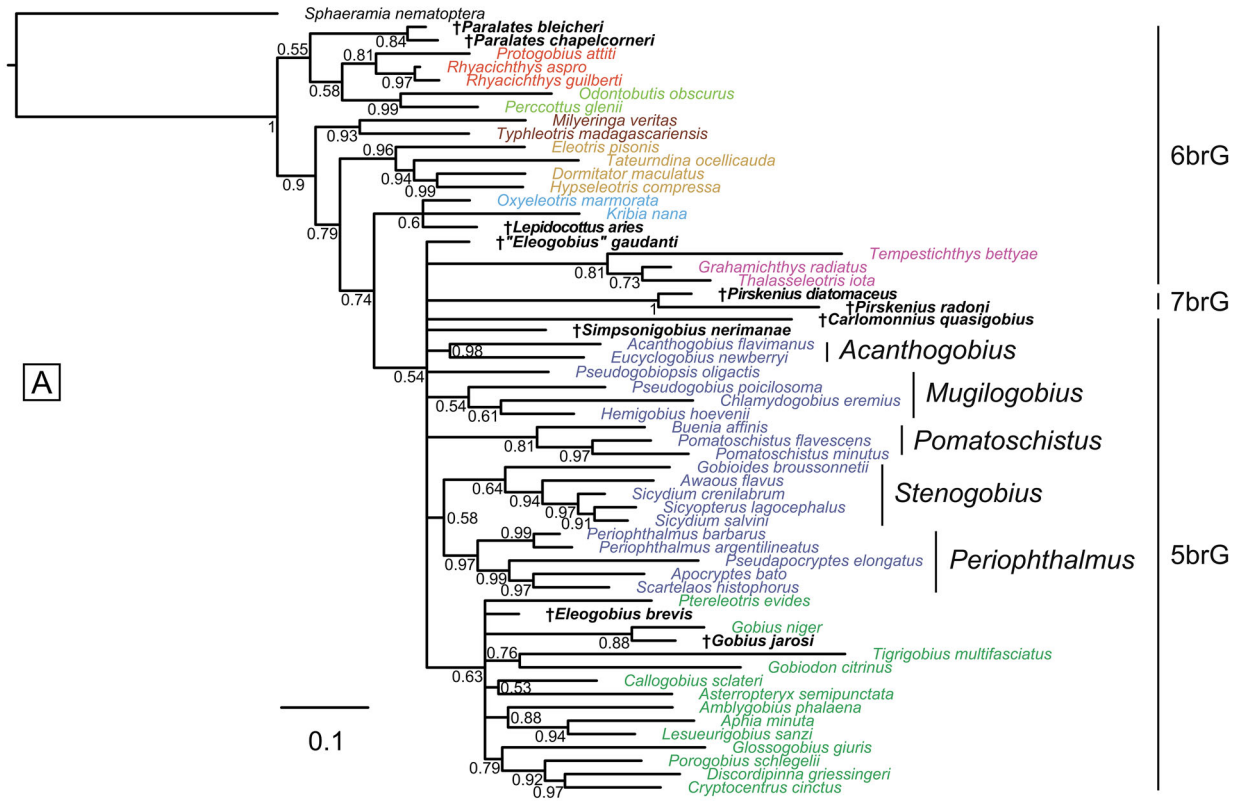
The BI reconstruction based on the combined molecular and morphological data is shown in Supplemental material Fig. S2A. The tree topology closely aligns with that derived from molecular data alone (Fig. 7A), except for the placement of *Pseudapocryptes elongatus*, which is now situated within the *Periophthalmus* lineage of the Oxudercidae, as anticipated. Furthermore, there is a notable increase in support for the Oxudercidae ($PP = 1$ vs 0.66), with high support values for all nodes within this family ($PP \geq 0.93$). The MP analysis based on the same data set yields a single most parsimonious tree (Supplemental material Fig. S2B). While the topology closely resembles the trees generated by the BI analyses using either molecular data or the total evidence data set, there is a decrease in support values for some clades.

Total evidence phylogenetic analyses including the fossil species

The results presented here for extant species demonstrate that a reliable phylogenetic placement of gobioid species cannot be achieved solely based on the current knowledge of morphological data. Therefore, we used the total evidence data set to scrutinize the phylogenetic relationships of the fossil species from Karalar Köyü.

The tree resulting from the BI analysis incorporating the extant species along with †*S. nerimanae* gen. et sp. nov. and the other nine fossil species included here is shown in Figure 8A. With the exception of the Oxudercidae, which is split into several clades, all extant families and the extinct family †Pirskeniidae are recovered as monophyletic. However, posterior probabilities notably decreased for the families Butidae ($PP = 0.6$ vs 1) and Gobiidae ($PP = 0.63$ vs 1) compared to the total evidence tree without fossils (see Fig. 8A vs Supplemental material Fig. S2A). The relationships between Thalasseleotrididae, Gobiidae and Oxudercidae are not resolved, while the relationships of the other families are consistent with those indicated by the molecular and total evidence trees. †*Simpsonigobius nerimanae* gen. et sp. nov. is positioned within the polytomy of Thalasseleotrididae, Gobiidae and Oxudercidae (Fig. 8A). In the MP analysis, the single most parsimonious tree, derived from the same data set, reveals poor

Figure 7. Results of the undated Bayesian inference analyses (50% majority-rule consensus trees). **A**, tree based on the extant species using solely published DNA data (ASDSF = 0.024051). **B**, tree based on the extant species using solely morphological characters (ASDSF = 0.005029). Values indicate posterior probabilities; scale bars show average number of substitutions per site (A) and character changes per character (B), respectively. ASDSF, average standard deviation of split frequencies between two independent runs. For sources of molecular data see Supplemental material Table S4.



support for deeper nodes (Supplemental material Fig. S3). While the relationships between extant families align with those in the BI tree, the Gobiidae is not resolved as monophyletic, whereas the Oxudercidae is. †*Simpsonigobius nerimanae* gen. et sp. nov. is positioned within the Oxudercidae, and the *Mugilogobius* lineage, but none of these groups receive strong support (BS < 70%) (Supplemental material Fig. S3).

Due to the severe decrease in support values when incorporating all 10 fossil taxa, we performed five additional BI analyses, each involving only one or two fossil taxa at a time, namely: (i) †*Simpsonigobius nerimanae* gen. et sp. nov. (Fig. 8B), (ii) †*Carlomonnius quasigobius* (Fig. 9A), (iii) both species of †*Pirskenius* (Fig. 9B), (iv) both species of †*Paralates* (Fig. 10A), and (v) †*Eleogobius brevis* and †*Eleogobius gaudanti* (Fig. 10B). In these analyses, all extant gobioid families appear monophyletic, with support values usually increased in comparison to the previous comprehensive analysis (shown in Fig. 8A). Furthermore, the established relationships of Thalasseleotrididae, Gobiidae and Oxudercidae are consistently recovered. The respective MP analyses (Supplemental material Figs S4, S5, S6) also demonstrate a clear increase in support values as compared to the previous MP analysis that included all 10 fossils (shown in Supplemental material Fig. S3).

When considering †*S. nerimanae* gen. et sp. nov. in the BI analysis with the reduced number of fossils, its placement within the Oxudercidae is now well supported (Fig. 8B, PP = 0.81). Similar to the MP analysis involving all 10 fossils, it is positioned within the *Mugilogobius* lineage, albeit with low support (PP = 0.55). In the MP analysis using the same reduced data set, a single most parsimonious tree is recovered (Supplemental material Fig. S4), in which Oxudercidae and Gobiidae is each monophyletic, and †*S. nerimanae* gen. et sp. nov. is placed within a well-supported 5brG clade (BS = 86%), as sister to Gobiidae + Oxudercidae.

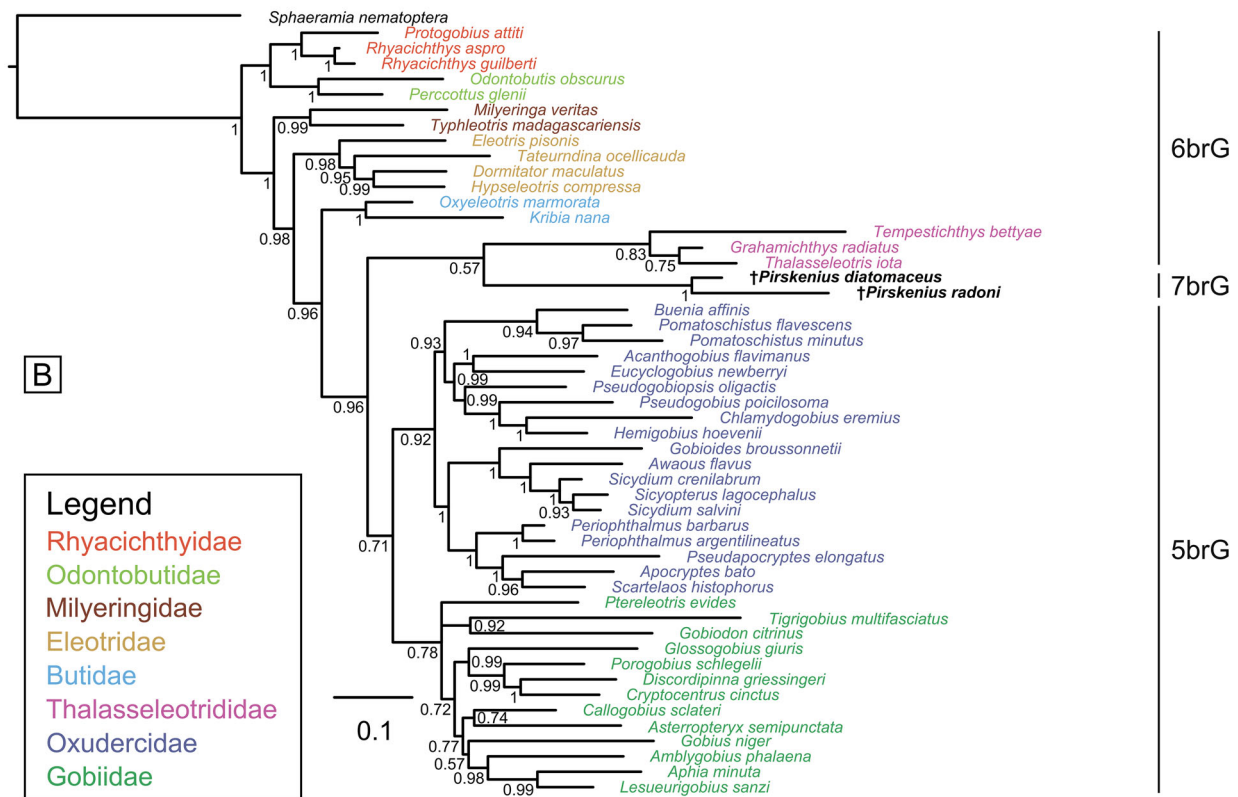
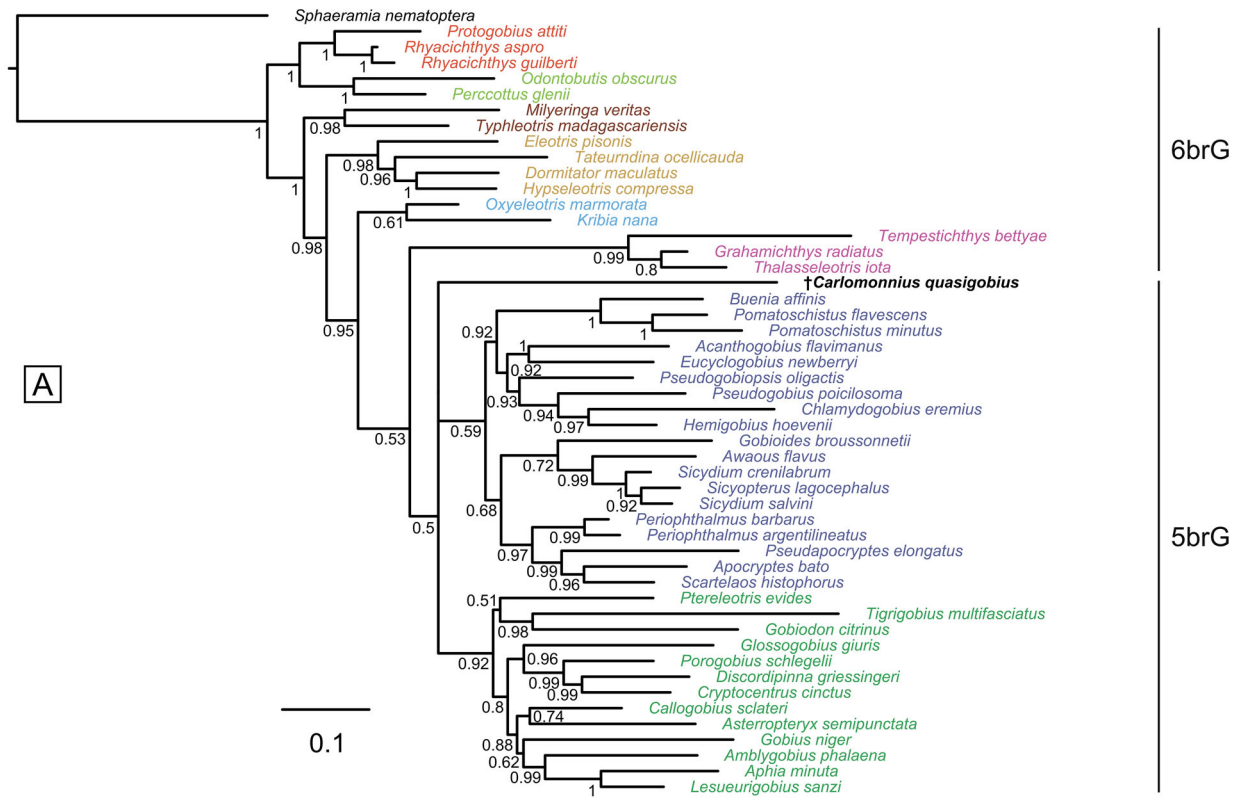
In the remaining four BI trees with reduced numbers of fossils, the positioning of most fossils aligns with the tree that includes all 10 fossils, but the individual trees are better resolved. †*Carlomonnius quasigobius* forms a polytomy with Gobiidae and Oxudercidae (PP = 0.5; Fig. 9A); the two †*Pirskenius* species constitute a clade (PP = 1) that is sister to the Thalasseleotrididae (PP =

0.57; Fig. 9B); †*Eleogobius brevis* is confidently placed within Gobiidae, which now has increased support (PP = 0.94; Fig. 10B) and †*Eleogobius gaudanti* is resolved as the sister taxon to Thalasseleotrididae (PP = 0.73; Fig. 10B). Variations in the placement of certain fossils compared to the tree with all fossils concern the clade of both †*Paralates* species (PP = 0.94), which is now positioned as the sister group to Rhyacichthyidae, albeit with low support (PP = 0.53; Fig. 10A). In the respective MP trees, the positions of the fossils can differ from those in the BI trees (Supplemental material Figs 5, 6), but support is consistently low, except for the monophyly of †*Pirskenius* (BS = 79%).

Total evidence phylogeny based on tip-dating

In the relaxed-clock total evidence phylogeny which includes the 10 fossils (Fig. 11), all families are resolved as monophyletic. Notably, the Oxudercidae, which was not resolved in the undated analysis with all 10 fossil species included (compare Figs 8A, 11), is now monophyletic. Additionally, the relationships between the families Thalasseleotrididae, Gobiidae and Oxudercidae are resolved, but the support values of these now monophyletic groups are low (PP of Oxudercidae = 0.51; PP of 5brG = 0.53). †*Carlomonnius quasigobius*, the oldest fossil species in the tree, is placed as sister to all other gobioids, but posterior probability is relatively low (PP of sister gobioid group = 0.64). The †*Pirskenius* clade (PP = 1) could not be confidently placed and consequently appears in a polytomy with the clade Odontobutidae + Rhyacichthyidae + †*Paralates*, as well as the 5brG + 6brG gobioid clade. The other fossil taxa occupy the same or congruent positions to those in the undated tree, but in most cases, they are better resolved or receive higher posterior probabilities (compare Fig. 8A vs Fig. 11). Even with all 10 fossil taxa included, the clock analysis recovers †*Simpsonigobius nerimanae* gen. et sp. nov. as a member of the Oxudercidae, consistent with the MP analysis involving all fossils (Supplemental material Fig. S3) and the BI and MP analyses with the reduced taxon set (Fig. 8B, Supplemental material Fig. S4). However, the support for the Oxudercidae is low (PP = 0.51). Moreover, our tip-dating analysis revealed as node ages for crown Gobioidaei 67.04 Ma (95% highest posterior density [HPD] 54.86–82.75 Ma), for crown Butidae 20.68 Ma (95% HPD 11.8–31.3 Ma), for crown

Figure 8. Results of the undated total evidence Bayesian inference analyses (50% majority-rule consensus trees). **A**, tree based on the extant species plus 10 fossil species (ASDSF = 0.017529). **B**, tree based on the extant species plus †*Simpsonigobius nerimanae* gen. et sp. nov. (ASDSF = 0.014561). ASDSF, average standard deviation of split frequencies between two independent runs. Values indicate posterior probabilities; scale bars depict average number of substitutions per site and character changes per character, respectively.



Thalasseleotrididae 18.58 Ma (95% HPD 12.26–27.54 Ma), for Gobiidae + Oxudercidae 38.49 Ma (95% HPD 29.71–46.52 Ma), for crown Gobiidae 34.13 Ma (95% HPD 26.97–43.51 Ma), and for crown Oxudercidae 34.83 Ma (95% HPD 27.10–43.36 Ma).

Results of the ancestral habitat reconstruction

As described in the ‘Materials and methods’ section, the best model was the one with ordered states and equal rates (graphically shown in [Supplemental material Fig. S7](#)), and this model was chosen for the stochastic character mapping analysis. For each of the Gobiidae and the Thalasseleotrididae, the most recent common ancestor is associated with marine or brackish to marine habitats, whereas for all other families and also for Gobiioidei in general, an association of the most recent common ancestor to brackish, freshwater, or both is reconstructed ([Fig. 12](#)). Only for Oxudercidae the most recent common ancestor is, according to this reconstruction, most likely associated to a combination of all three habitats.

Discussion

In the following sections, we investigate the possible relationship of †*Simpsonigobius* gen. nov. through a comparative morphological approach, and assess its concordance with the interpretation from our phylogenetic analyses. Furthermore, we discuss the results of our additional phylogenetic analyses, particularly in regard to the placement of the fossil taxa in comparison to where they were positioned in the earlier study by Gierl *et al.* (2022). Finally, we discuss our divergence time estimates and the reconstruction of ancestral habitats in light of the previous studies that relied solely on molecular data.

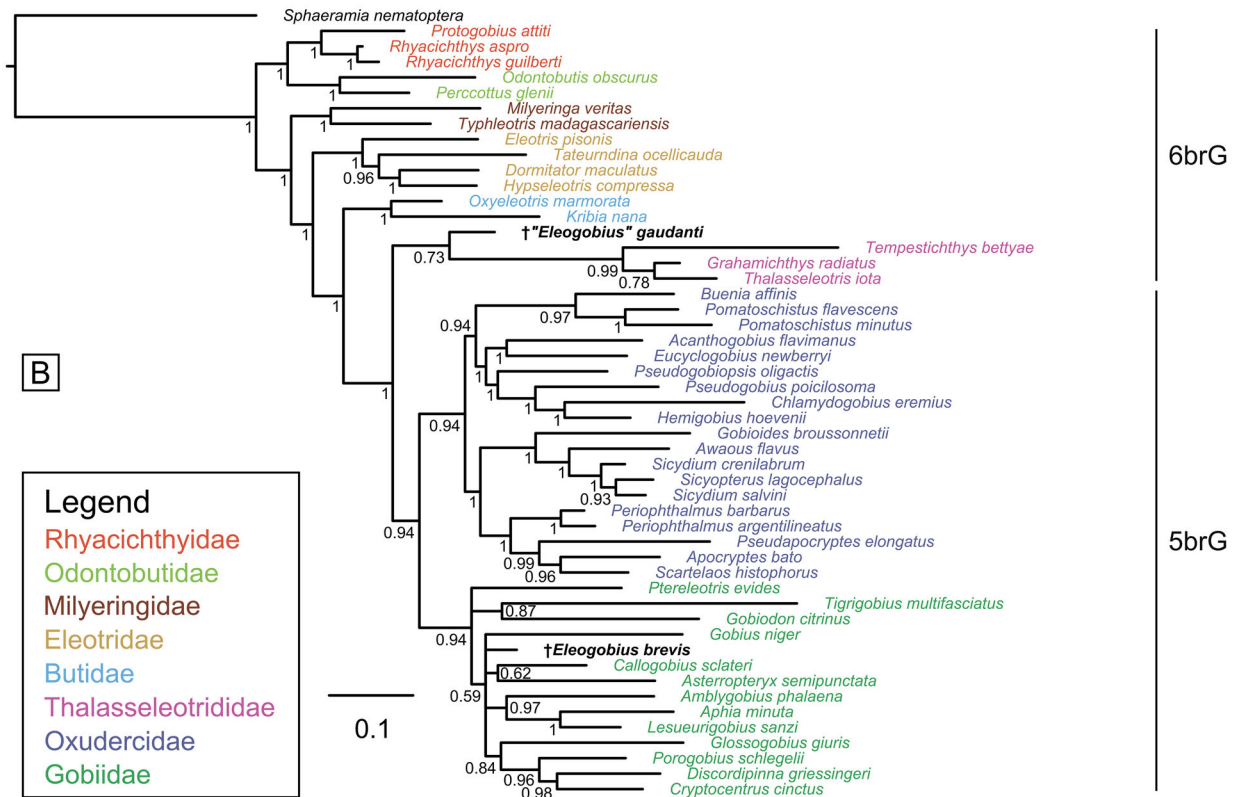
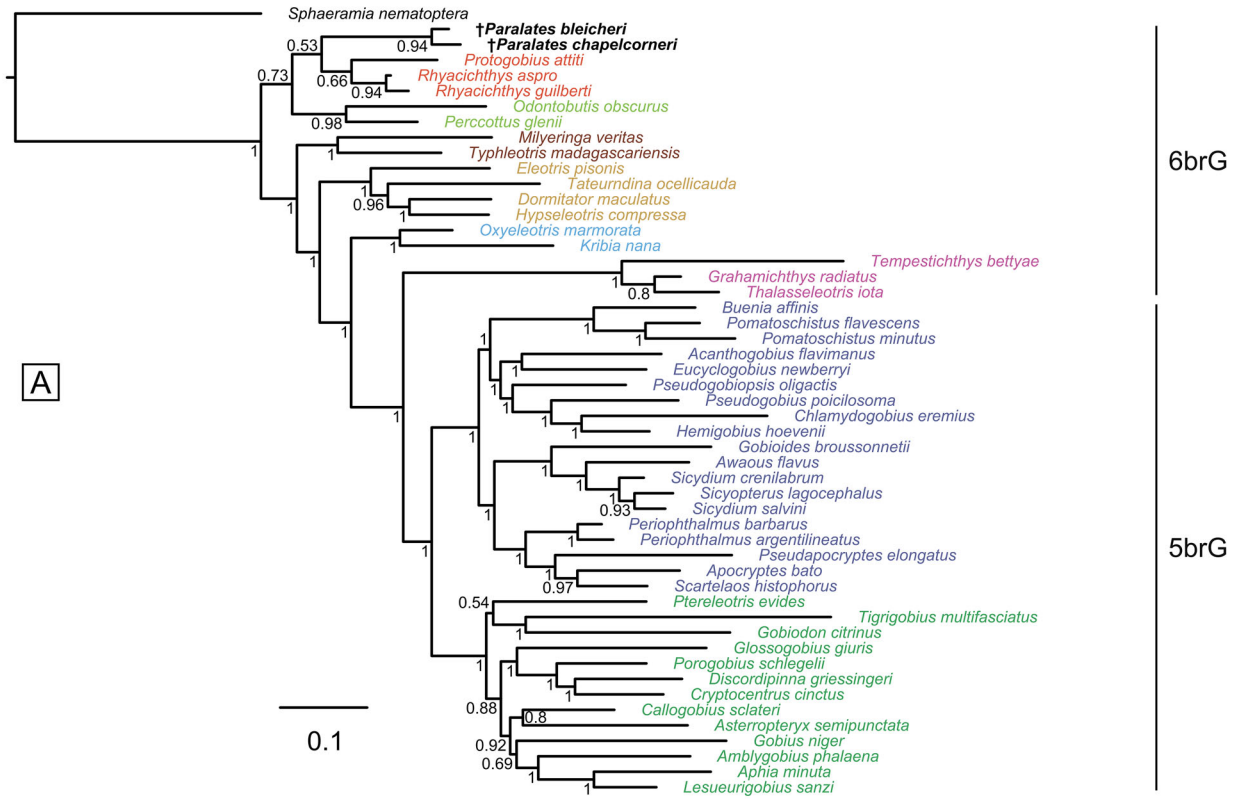
Comparative morphology

Exploring the relationship of †*Simpsonigobius* gen. nov. The set of characters that defines the Gobiioidei has been discussed for over a century (e.g. Patzner, 2011; Regan, 1911; Wiley & Johnson, 2010; Winterbottom,

1993). Some of these characters refer to soft tissue, but others are osteological, and three of the latter can be recognized in †*S. nerimanae* gen. et sp. nov., i.e. (i) the absence of parietal bones (Hoese, 1984; Regan, 1911; Springer, 1983); (ii) the presence of a fenestra between preopercle and symplectic, bordered by hyomandibular and quadrate ([Fig. 5A](#)) (Gosline, 1955; Harrison, 1989; P. J. Miller, 1973); and (iii) a caudal skeleton in which hypurals 1 + 2 have fused to form a plate, hypurals 3 + 4 are fused to each other and to the terminal centrum, and hypural 5 is autochthonous and small ([Fig. 6B](#)) (Birdsong, 1975; Hoese, 1984). Accordingly, the assignment of †*S. nerimanae* gen. et sp. nov. to the Gobiioidei is unequivocal.

Among the Gobiioidei, the Gobiidae + Oxudercidae clade (= 5brG) has been recognized as sister to the Thalasseleotrididae based on both morphological (A. C. Gill & Mooi, 2012) and molecular (Agorreta *et al.*, 2013; Thacker *et al.*, 2015) analyses. There are five morphological synapomorphies for the clade comprising these three families (see A. C. Gill & Mooi, 2012), which, however, are not discernible in †*S. nerimanae* gen. et sp. nov. Nevertheless, the extant members of the three families display several further characteristics that usually do not occur in the other families (Birdsong *et al.*, 1988; A. C. Gill & Mooi, 2012; Hoese, 1984; Hoese & Gill, 1993). Three of those can be recognized in the new fossil taxon from Karalar Köyü: (i) absence of the endopterygoid ([Fig. 5A](#)), (ii) presence of an interneural gap, and (iii) a palatine with an at least slightly ‘T’-shaped head ([Fig. 5A](#)). It is worth noting that the palatine of †*S. nerimanae* gen. et sp. nov. is conspicuously similar to the palatine of the thalasseleotridid *Tempestichthys bettyae* (see Goatley & Tornabene, 2022), and also shows a slight resemblance to the clearly ‘T’-shaped palatine (with distinct maxillary and ethmoid processes) of the Gobiidae and Oxudercidae (other families usually have an ‘L’-shaped palatine, with a reduced ethmoid process; see Regan, 1911; Reichenbacher *et al.*, 2020). In conclusion, the presence of the three traits suggests that †*S. nerimanae* gen. et sp. nov. may belong to the clade Thalasseleotrididae + (Gobiidae + Oxudercidae). This proposition is consistent with the outcome of our BI analysis including all 10 fossils, which positioned †*S. nerimanae* gen. et sp. within the polytomy of Thalasseleotrididae, Gobiidae and Oxudercidae ([Fig. 8A](#)).

Figure 9. Results of the undated total evidence Bayesian inference analyses (50% majority-rule consensus trees). Tree based on the extant species. **A**, plus †*Carlomonnius quasigobius* (ASDSF = 0.007185). **B**, plus †*Pirskenius diatomaceus* and †*Pirskenius radoni* (ASDSF = 0.018613). ASDSF, average standard deviation of split frequencies between two independent runs. Values indicate posterior probabilities; scale bars depict average number of substitutions per site and character changes per character, respectively.



Arguments for and against a relationship with the Thalasseleotrididae. The sole synapomorphy of the family Thalasseleotrididae is a membrane that lies between the hyoid bar and ceratobranchial 1 (A. C. Gill & Mooi, 2012), which is unlikely to be preserved in a fossil, and is not conserved in †*Simpsonigobius* gen. nov. However, in addition to the palatine with the weakly ‘T’-shaped head, †*Simpsonigobius* gen. nov. also shares another distinctive feature with the Thalasseleotrididae: the presence of separated pelvic fins, evident from the clear distance between their bases. This characteristic suggests an affinity with the Thalasseleotrididae rather than with Gobiidae and Oxudercidae, as fusion of the pelvic fins by a membrane represents the derived condition in Gobiidae and Oxudercidae, although exceptions exist (see Hoese and Gill, 1993; Regan, 1911).

On the other hand, Thalasseleotrididae possess six branchiostegal rays, while the presence of five branchiostegal rays represents the derived condition of Gobiidae + Oxudercidae and is also observed in †*Simpsonigobius* gen. nov. Furthermore, all four extant thalasseleotridid species, i.e. *Thalasseleotris iota* Hoese and Roberts, 2005, *Th. adela* Hoese and Larson, 1987, *Grahamichthys radiatus* (Valenciennes, 1837) and *Tempestichthys bettyae*, exhibit an anal fin with either one ray fewer or an equal number of rays compared to the second dorsal fin, whereas †*S. nerimanae* gen. et sp. nov. has one additional ray in the anal fin. Moreover, the premaxilla in Thalasseleotrididae bears a distinct postmaxillary process (Goatley & Tornabene, 2022, unknown for *Th. adela*), whereas †*S. nerimanae* gen. et sp. nov. has a premaxilla with either a weakly developed postmaxillary process or none at all (Fig. 5C). Additionally, the otoliths of Thalasseleotrididae lack a posterodorsal projection (Schwarzahns, 2019, figs 99.9–11), whereas the otoliths of †*S. nerimanae* gen. et sp. nov. do have such a projection (Fig. 4B). Altogether, the character combination seen in †*S. nerimanae* gen. et sp. nov. does not imply its close relationship with the family Thalasseleotrididae.

Arguments for a relationship with the 5brG clade and the Oxudercidae. The combination of characters observed in †*S. nerimanae* gen. et sp. nov. (five branchiostegal rays, presence of interneural gap, absence of endopterygoid), suggests its association with the 5brG clade (Gobiidae + Oxudercidae) (Akihito *et al.*, 2000;

Hoese, 1984). Unfortunately, only a few characters allow for the classification of a fossil gobioid into either Gobiidae or Oxudercidae (Reichenbacher *et al.*, 2018). One such characteristic is the strength of the postmaxillary process of the premaxilla, as this process is typically well developed in Gobiidae but not in Oxudercidae (McKay & Miller, 1997; Thacker, 2013). Notably, within the ‘sand goby’ group of the Oxudercidae, this process is usually entirely absent, except in females of *Pomatoschistus flavescens* (Fabricius, 1779), where it may be weakly developed (McKay & Miller, 1997). Another notable characteristic is the presence of an additional ray in the anal fin (compared to D2), which has been documented only in certain species of the Oxudercidae in which it appears to be a derived character (Pezold, 2004). Given that †*S. nerimanae* gen. et sp. nov. displays a premaxilla with a weak or absent postmaxillary process (Fig. 5C) and an anal fin with one ray more than in the second dorsal fin (Fig. 6A2), its classification within the Oxudercidae appears to be justified based on comparative morphology. Additionally, it is worth noting that †*S. nerimanae* gen. et sp. nov. does not fit within the sand goby group (to which it initially was assigned by Rückert-Ülkümen, 2000), as species in this group typically exhibit a higher number of vertebrae (30–33; see Birdsong *et al.*, 1988; McKay & Miller, 1997) than seen in †*Simpsonigobius* gen. nov. which possesses 26–27 vertebrae. Also, the otoliths of sand gobies are quite different from those of the fossil species, as they usually do not possess a posterodorsal projection (see Gierl *et al.*, 2018, fig. 3; Gut *et al.*, 2020, fig. 6).

In conclusion, †*Simpsonigobius* gen. nov. shares two phylogenetically informative morphological characters with the Oxudercidae, suggesting its classification within this family. This is consistent with the outcome of our undated and dated total evidence phylogenetic analyses, as depicted in Figures 8B and 11, and reinforces the credibility of our total evidence approach.

Discussion of phylogenetic results based on our updated matrix

Trees of extant taxa using molecular and total evidence data. The following refers to the results of the BI trees. The reconstructed phylogenies based on the

← **Figure 10.** Results of the undated total evidence Bayesian inference analyses (50% majority-rule consensus trees). Tree based on the extant species. **A**, plus †*Paralates bleicheri* and †*Paralates chapelcorneri* (ASDSF = 0.003994). **B**, plus †*Eleogobius brevis* and †*Eleogobius gaudanti* (ASDSF = 0.008386). ASDSF, average standard deviation of split frequencies between two independent runs. Values indicate posterior probabilities; scale bars depict average number of substitutions per site and character changes per character, respectively.

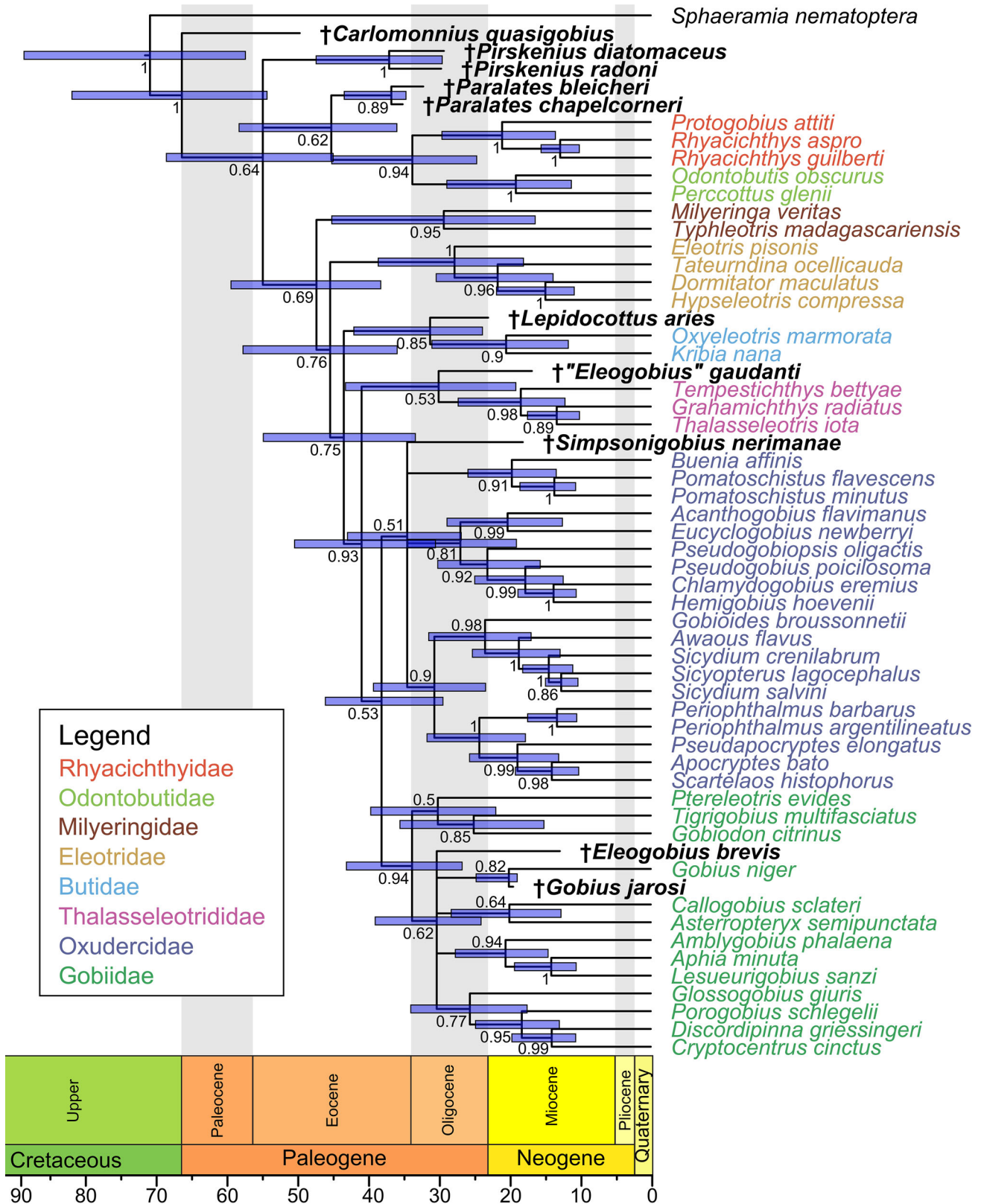


Figure 11. Tip-dated, relaxed-clock total evidence Bayesian inference phylogeny (fossilized birth–death tree model) including all 10 fossil species (ASDSF = 0.028530). ASDSF, average standard deviation of split frequencies between two independent runs. Numbers at nodes depict posterior probability, node bars indicate the 95% highest posterior density for divergence times. Scale axis in Ma; chronostratigraphic chart following Cohen et al. (2022).

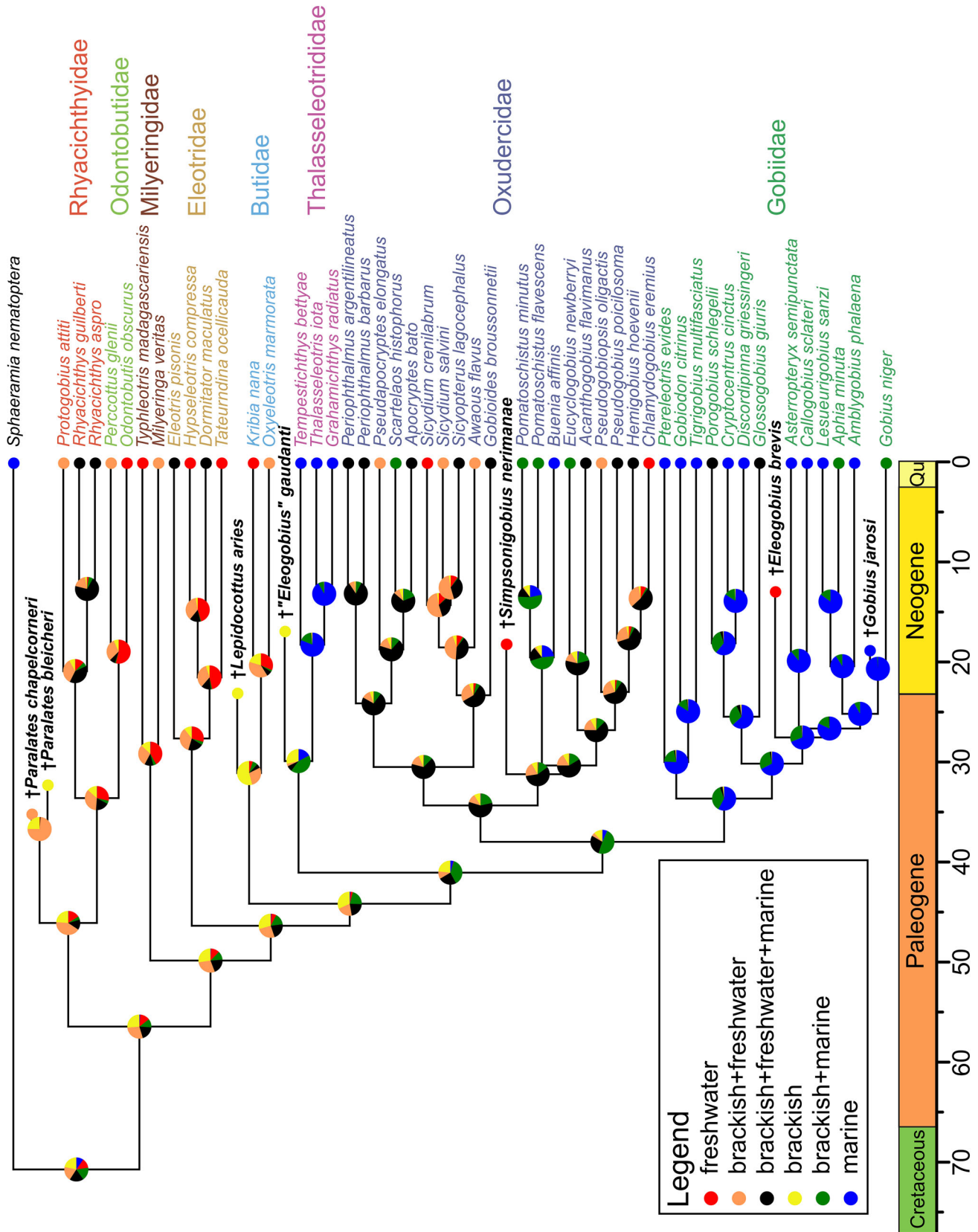


Figure 12. Ancestral habitat reconstruction, based on stochastic character mapping, with ancestral states sampled from 10,000 simulations. Pie charts depict the posterior probability of each habitat type at the respective node. Scale axis in Ma; chronostratigraphic chart following Cohen *et al.* (2022).

molecular data and total evidence data derived from the extant species in our new matrix (Fig. 7A, Supplemental material Fig. S2A) are consistent with previously published phylogenies that were based on larger data sets (e.g. Agorreta et al., 2013; Thacker et al., 2015). This implies that our extant taxon set, like that compiled by Gierl et al. (2022), is capable of yielding a molecular ‘backbone’ that facilitates the placement of fossils in a phylogenetic context. The fact that the extant genus *Sicydium* Valenciennes, 1837 could not be resolved as monophyletic (Figs 7–11) is consistent with the tree published by Tornabene et al. (2013, fig. 2), and is therefore not an artefact of our choice of taxon set. Notably, *Sicydium* has been recovered as monophyletic in the MP analyses (Supplemental material Figs S1A, S2B), which emphasizes the value of using different phylogenetic reconstruction methods. The fact that *Pseudapocryptes elongatus* occurred in a polytomy with the rest of the Oxudercidae and the Gobiidae when only the molecular data set was used (Fig. 7A), while the total evidence data set convincingly placed the species within the Oxudercidae (Supplemental material Fig. S2A), raised another concern. However, this issue can be readily explained. Only a single gene (*cytb*, see Supplemental material Table S4) was available for *Ps. elongatus*, which emphasizes the value of using multiple molecular markers for a robust phylogeny. Overall, the total evidence-based tree reconstruction of the 48 extant ingroup taxa (Supplemental material Fig. S2A) clearly benefited from the use of both molecular and morphological data, since support values for nearly all nodes increased relative to those obtained from molecular or morphological data alone (Fig. 7A, B). This is in agreement with previous studies using total evidence data sets for other vertebrate groups (see Beck et al., 2023 and references therein).

Trees of extant and fossil taxa using total evidence data. In the undated BI analysis (Figs 8–10), the phylogenetic positioning of the fossil species reveals that six of them exhibit results consistent with those reported by Gierl et al. (2022). The †Pirskeniidae (two species) appear monophyletic and are not resolved within the tree containing all 10 fossils (nor in our clock tree). However, when introduced as sole fossils into the tree of extant taxa (Fig. 9B), †Pirskeniidae is resolved as sister to the Thalasseleotrididae, albeit with low support. As in Gierl et al. (2022), †*Eleogobius brevis* and †‘*E. gaudanti*’ are paraphyletic, and †‘*E. gaudanti*’ is resolved in the tree containing †*Eleogobius* as the sole fossil taxon as a stem member of Thalasseleotrididae (Fig. 10B, PP = 0.73). However, this positioning should be considered with caution, as the presence of six branchiostegal rays in †‘*E. gaudanti*’ could be neither confirmed nor disproven in our

study (see also Bradić-Milinović et al., 2019). Notably, and opposite to Gierl et al. (2022), †*E. brevis* is consistently resolved as a member of Gobiidae, both in the tree with all fossils (Fig. 8A, PP = 0.63) and in the tree containing †*Eleogobius* as the sole fossil taxon (Fig. 10B, PP = 0.94). Finally, as in Gierl et al. (2022), †*Lepidocottus aries* (Agassiz, 1839) is resolved as a stem member of the Butidae (Fig. 8A, PP = 0.6), and †*Gobius jarosi* Příkryl & Reichenbacher, 2018 in Reichenbacher et al. (2018) as sister to *G. niger* Linnaeus, 1758 (Fig. 8A, PP = 0.88).

Discrepancies between our BI analyses and those of Gierl et al. (2022) using single fossil taxa relate to the following: (i) †*Carlomonnius quasigobius* occurs in a very weakly supported polytomy with Oxudercidae and Gobiidae (Fig. 9A, PP = 0.5), but emerges as a member of Butidae in Gierl et al. (2022); (ii) †*Paralates* (two species) is recovered as monophyletic and positioned as sister to Rhyacichthyidae (Fig. 10A) (vs not monophyletic and not resolved in Gierl et al., 2022).

A striking outcome of the previous total evidence analyses was that the topology of the total evidence tree collapsed considerably when all 10 fossil species were included (Gierl et al., 2022, fig. 5B). Following our modifications of the previous morphological matrix, and the newly added extant taxa, the total evidence tree in the present study did not collapse as before (Fig. 8A): The Butidae are resolved as sister to Thalasseleotrididae + 5brG (vs not resolved in Gierl et al., 2022, fig. 5B) and the Gobiidae are monophyletic (vs not in Gierl et al., 2022, fig. 5B). Additionally, the results of the trees containing single fossil taxa are highly congruent, although usually better resolved, compared to the tree with all fossil taxa added (compare Figs 8A, 9, 10). This is in line with the outcome of a recent investigation, albeit one dealing with completely different fossils (Cambrian Bilateria), which also showed that amendments of morphological data sets can lead to a significantly improved phylogenetic framework (Bekkouche & Gąsiorowski, 2022).

Age divergences inferred from the tip-dated total evidence phylogeny. Previous temporal frameworks for gobioid evolution were exclusively based on a molecular Bayesian framework in which fossils were used solely for node dating (e.g. Thacker, 2015; Thacker et al., 2023). Our study is the first that has analysed fossil and extant gobioid species simultaneously with the aim of deriving a species-level total evidence phylogeny together with dating of the tree. Notably, our inferred median divergence age for the split between †*Carlomonnius* and crown Gobiioidei (67.04 Ma) is only slightly younger than the age that Thacker et al. (2023) inferred for crown Gobiioidei (69.25 Ma). Likewise, our inferred median divergence age for crown Butidae

(20.68 Ma) is only slightly younger than the inferred age for crown Butidae in Thacker *et al.* (2023) (23.53 Ma). Also, the ages for Gobiidae + Oxudercidae (not included in Thacker *et al.* 2023) estimated by Jeon *et al.* (2021) are remarkably similar to the ages of our study (node ages in Jeon *et al.* for Gobiidae + Oxudercidae: 38.66 Ma, 95% HPD 30.02–47.51 Ma, for Gobiidae: 34.00 Ma, 95% HPD 26.00–42.36 Ma, for Oxudercidae: 35.61 Ma, 95% HPD 27.72–44.27 Ma). An earlier study by Thacker (2014), however, had estimated clearly older median node ages for Butidae (57 Ma, vs 23.5 Ma in Thacker *et al.*, 2023, vs 20.7 Ma in our study), Gobiidae + Oxudercidae (55 Ma, vs 38.7 Ma in Jeon *et al.*, 2021, vs 38.5 Ma in our study), crown Gobiidae (49 Ma vs 34.0 Ma in Jeon *et al.*, 2021, vs 34.13 Ma in our study) and crown Oxudercidae (48 Ma, vs 35.6 Ma in Jeon *et al.*, 2021, vs 34.8 Ma in our study). One might think that the older ages estimated by Thacker (2014) could be biased due to availability of only a few fossil calibration points at that time. However, the fact that Jeon *et al.* (2021) used a single fossil taxon (†*Carlomonnus*) for their time calibration does not support this idea. Another possibility is that the taxonomic unit under study plays a role. The study of Thacker (2014) encompassed both Gobioidae and cardinal fishes (Apogonoidei, Kurtidae), whereas Thacker *et al.* (2023) and Jeon *et al.* (2021) each focused on a distinct gobioid family (Eleotridae in Thacker *et al.*, 2023, Oxudercidae in Jeon *et al.*, 2021) for which they utilized a very comprehensive taxon set. It thus seems that a focus on a specific gobioid family (or gobioid entity) coupled with the use of a comprehensive taxon set can lead to time calibrations that conform well to the fossil record. This is reinforced by the late Eocene age (*c.* 35 Ma) for the node of the Oxudercidae, as estimated in our study and by Jeon *et al.* (2021), as the oldest oxudercid fossils currently known are otoliths from the Oligocene (early Chattian, *c.* 26–27 Ma, Reichenbacher & Schwarz, 1997).

In this context, it is interesting to note that a previous study dealing with another teleost group (Tetraodontiformes) in a total evidence phylogenetic framework found that tip-dating generally provided *older* ages than node dating (*i.e.* the opposite to what we found), but that tip-dating precision increased as more fossils were included (Arcila *et al.*, 2015). In addition, these authors discovered that the precision of node ages inferred from tip-dating improves even more when the fossils included are close to the considered node. As this is the approach adopted here, and also because our inferred age for crown Butidae, to which Thalasseleotridae and 5brG are sister, is only slightly younger than the corresponding age in Thacker *et al.*

(2023), we assume that our inferred median divergence ages give reasonable temporal estimates for the Butidae, 5brG, Gobiidae and Oxudercidae.

Ancestral habitat reconstruction. While Thacker and Hardman (2005) previously noted that basal gobioids frequently inhabit fresh water and estuaries, subsequent studies employing ancestral habitat reconstruction analysis for Gobioidae indicate a prevailing trend of freshwater ancestry within the group (Jeon *et al.*, 2021; Thacker, 2009, 2014). Additionally, these studies revealed singular invasions into brackish and marine environments among the 'less-derived' Gobioidae (6brG), with an evolutionary trend towards brackish and estuarine habitats in the Oxudercidae, and a notable preference for marine environments in the Gobiidae.

For the first time, we have integrated fossil taxa and their habitat data into an ancestral habitat reconstruction analysis, and utilized stochastic character mapping to illustrate the likelihoods of the reconstructed states at the nodes (Fig. 12). Our analysis aligns with prior works regarding the invasions of marine habitats by derived gobioids (5brG). Additionally, we observe a transition towards exclusively marine environments within crown Thalasseleotridae, a group included in such an analysis for the first time.

Discrepancies from prior findings concern the initial condition at the root of gobioids, which varies significantly in our study. Our results reveal a higher likelihood for broader salinity tolerances (euryhaline or a combination of freshwater + brackish) or favouring brackish conditions. This difference likely arises from the inclusion of †*Paralates bleicheri*, associated with brackish conditions (Gaudant, 1979), and †*Paralates chapelcorneri*, for which freshwater to brackish conditions can be assumed (Gaudant & Quayle, 1988).

Moreover, discerning the habitat association of early-splitting extant taxa holds paramount importance in inferring the ancestral state at the root. In previous analyses, either the positioning of exclusively freshwater species near the root remains questionable (*e.g.* *Milyeringa veritas* Whitley, 1945 within Odontobutidae in Thacker, 2009), or the habitat classification of early-splitting taxa itself (*e.g.* *Rhyacichthys aspro* (Valenciennes, 1837) exclusively in fresh water according to Jeon *et al.*, 2021). Considering the prevalence of combined habitat types among early-splitting extant taxa in the results of our analysis, it seems evident that the Gobioidae ancestor likely did not inhabit exclusively freshwater environments.

Conclusions

The results of this study reveal that the fossil gobioid from the Lower Miocene of Karalar Köyü, western Turkey, previously described as ‘*Pomatoschistus* cf. *bleicheri* Sauvage, 1883’, cannot be a member of the extant genus *Pomatoschistus*, and is also clearly different from †*Paralates bleicheri* Sauvage, 1883 (now the valid name for *Pomatoschistus bleicheri* (Sauvage, 1883)). Rather, it represents a new extinct gobioid genus and species, which we named †*Simpsonigobius nerimanae* gen. et sp. nov. Furthermore, we were able to resolve †*S. nerimanae* gen. et sp. nov. as a member of the present-day family Oxudercidae, in both an undated and a tip-dated total evidence-based phylogenetic framework. Our results highlight the potential of this approach to infer the phylogenetic relationships of gobioid fossils that would have been left as *incertae sedis* if comparative morphology alone had been used.

The total evidence matrix used here is an amended version of the morphological matrix previously published by Gierl et al. (2022), to which we added a new taxon set (19 species). The matrix now comprises 48 extant and 10 fossil gobioid species, 48 morphological characters, and 6349 base pairs from five genes (vs 29 extant and 10 fossil gobioid species, 48 morphological characters, 6271 base pairs from five genes in the previous study). Our phylogenetic results clearly demonstrate that both the amendments and the expansion of the set of taxa contributed to a significant improvement in the phylogenetic resolution at species, lineage and family levels, which will be valuable for future phylogenetic analyses of gobioid fossils.

Our study is the first to analyse fossil and extant gobioid species simultaneously in a tip-dated total evidence framework with the aim of inferring a species-level phylogeny together with dating of the tree. From the tip-dating analysis we inferred a late Eocene median divergence age for Oxudercidae (34.8 Ma) and Gobiidae (34.1 Ma). Comparison with previous age estimates for crown Gobioidae and crown Butidae that were based on molecular data, and in which fossils served solely for node dating, reveals that our corresponding age estimates are only about 3 million years younger than had been estimated before. This, and the congruence with the fossil record, corroborates our inferred ages for the Butidae, 5brG, Gobiidae and Oxudercidae. Finally, for the first time, we estimated ancestral habitat types utilizing a dated tree that included extinct species. The results reveal an ancestral lineage of Gobioidae not confined solely to freshwater habitats, but rather adapted to a wider spectrum of salinity, including brackish conditions.

Data availability statement

All relevant data are provided within the manuscript and the supplementary tables. The latter can be found online at <https://figshare.com/s/1542a1b91c384c6ae913>. The tree files underlying the results shown in Figs 7–11 and Figs S1–6 are also available at figshare; see <https://figshare.com/s/1c886af82e54c062531f>.

Authorship contribution statement

Moritz Dirnberger: conceptualization, methodology, formal analysis, investigation, resources, writing – original draft, review and editing, visualization. **Elena Bauer:** methodology, formal analysis, investigation, writing – review, visualization. **Bettina Reichenbacher:** conceptualization, methodology, formal analysis, investigation, resources, writing – original draft, review and editing, visualization.

Acknowledgements

We are grateful to James Maclaine (NHMUK) for access to the specimens of the NHMUK fish collection, and to Brett Clark (NHMUK) for conducting the micro-CT scan of *Pomatoschistus minutus* used in this study. We are indebted to Ulrich Schliewen (SNSB-ZSM, Munich) for providing access to the Faxitron System and to the fish specimens kept in the SNSB-ZSM collection, and also to Alexander Cerwenka (SNSB-ZSM, Munich) and Jana Schmid (LMU Munich) for technical support in processing micro-CT data with Amira. We are grateful to Dirk Erpenbeck (LMU Munich) and Lukas Dirnberger (TUM, Munich) for providing many helpful comments and to Paul Hardy (Düsseldorf) for critical reading of the manuscript. Finally, we thank Werner Schwarzahns (Hamburg) and an anonymous reviewer for their detailed reviews of an earlier version of this manuscript, and Associate Editor Erin Maxwell (SMNS) and co-Editor in Chief Zerina Johanson for their constructive advice during the revision.

Disclosure Statement

No potential conflict of interest was reported by the author(s).

Supplemental material

Supplemental material for this article can be accessed here: <https://doi.org/10.1080/14772019.2024.2340498>.

ORCID

Moritz Dirnberger  <http://orcid.org/0000-0002-2844-3554>

Elena Bauer  <http://orcid.org/0009-0000-0681-760X>

Bettina Reichenbacher  <http://orcid.org/0000-0001-6678-5080>

References

- Agassiz, L. (1839–1844). *Recherches sur les poissons fossiles* (Vol. 4). Petitpierre.
- Agiadi, K., Giamali, C., Girone, A., Moissette, P., Koskeridou, E., & Karakitsios, V. (2020). The Zanclean marine fish fauna and palaeoenvironmental reconstruction of a coastal marine setting in the eastern Mediterranean. *Palaeobiodiversity and Palaeoenvironments*, 100(3), 773–792. <https://doi.org/10.1007/s12549-019-00404-4>
- Agiadi, K., Girone, A., Koskeridou, E., Moissette, P., Cornée, J.-J., & Quillévéré, F. (2018). Pleistocene marine fish invasions and paleoenvironmental reconstructions in the eastern Mediterranean. *Quaternary Science Reviews*, 196, 80–99. <https://doi.org/10.1016/j.quascirev.2018.07.037>
- Agiadi, K., Vasileiou, G., Koskeridou, E., Moissette, P., & Cornée, J.-J. (2019). Coastal fish otoliths from the early Pleistocene of Rhodes (eastern Mediterranean). *Geobios Memoire Special*, 55, 1–15. <https://doi.org/10.1016/j.geobios.2019.06.006>
- Agorreta, A., San Mauro, D., Schliewen, U., Van Tassell, J. L., Kovacic, M., Zardoya, R., & Rüber, L. (2013). Molecular phylogenetics of Gobioidae and phylogenetic placement of European gobies. *Molecular Phylogenetics and Evolution*, 69(3), 619–633. <https://doi.org/10.1016/j.ympev.2013.07.017>
- Akihito, Iwata, A., Kobayashi, T., Ikee, K., Imanishi, T., Ono, H., Umehara, Y., Hamamatsu, C., Sugiyama, K., Ikeda, Y., Sakamoto, K., Fumihito, A., Ohno, S. & Gojobori, T. (2000). Evolutionary aspects of gobioid fishes based upon a phylogenetic analysis of mitochondrial cytochrome *b* genes. *Gene*, 259(1–2), 5–15. [https://doi.org/10.1016/S0378-1119\(00\)00488-1](https://doi.org/10.1016/S0378-1119(00)00488-1)
- Altekar, G., Dwarkadas, S., Huelsenbeck, J. P., & Ronquist, F. (2004). Parallel metropolis coupled Markov chain Monte Carlo for Bayesian phylogenetic inference. *Bioinformatics*, 20(3), 407–415. <https://doi.org/10.1093/bioinformatics/btg427>
- Arcila, D., Pyron, R. A., Tyler, J. C., Ortí, G., & Betancur-R, R. (2015). An evaluation of fossil tip-dating versus node-age calibrations in tetraodontiform fishes (Teleostei: Percomorphaceae). *Molecular Phylogenetics and Evolution*, 82(Part A), 131–145. <https://doi.org/10.1016/j.ympev.2014.10.011>
- Bajpai, S., & Kapur, V. V. (2004). Oldest known gobiids from Vastan Lignite Mine (early Eocene), Surat district, Gujarat. *Current Science*, 87(4), 433–435.
- Bannikov, A. F., & Carnevale, G. (2016). †*Carlomonnius quasigobius* gen. et sp. nov.: The first gobioid fish from the Eocene of Monte Bolca, Italy. *Bulletin of Geosciences*, 91, 13–22. <https://doi.org/10.3140/bull.geosci.1577>
- Bauer, E., Cerwenka, A. F., Schliewen, U., & Reichenbacher, B. (in review). New osteological characteristics identify the first stem sleeper goby (Gobioidae, Odontobutidae) from the Upper Eocene. *Papers in Palaeontology*.
- Beck, R. M. D., de Vries, D., Janiak, M. C., Goodhead, I. B., & Boubli, J. P. (2023). Total evidence phylogeny of platyrrhine primates and a comparison of undated and tip-dating approaches. *Journal of Human Evolution*, 174, 103293. <https://doi.org/10.1016/j.jhevol.2022.103293>
- Bekkouche, N., & Gąsiorowski, L. (2022). Careful amendment of morphological data sets improves phylogenetic frameworks: Re-evaluating placement of the fossil *Amiskwia sagittiformis*. *Journal of Systematic Palaeontology*, 20(1), 1–14. <https://doi.org/10.1080/14772019.2022.2109217>
- Bellon, H., Bůžek, Č., Gaudant, J., Kvaček, Z., & Walter, H. (1998). The České Středoohří magmatic complex in Northern Bohemia 40K–40Ar ages for volcanism and biostratigraphy of the Cenozoic freshwater formations. *Newsletters on Stratigraphy*, 36(2–3), 77–103. <https://doi.org/10.1127/nos/36/1998/77>
- Benson, D. A., Cavanaugh, M., Clark, K., Karsch-Mizrachi, I., Lipman, D. J., Ostell, J., & Sayers, E. W. (2013). GenBank. *Nucleic Acids Research*, 41(Database issue), D36–42. <https://doi.org/10.1093/nar/gks1195>
- Berger, J.-P., Reichenbacher, B., Becker, D., Grimm, M., Grimm, K., Picot, L., Storni, A., Pirkenseer, C., & Schaefer, A. (2005). Eocene–Pliocene time scale and stratigraphy of the Upper Rhine Graben (URG) and the Swiss Molasse Basin (SMB). *International Journal of Earth Sciences*, 94(4), 711–731. <https://doi.org/10.1007/s00531-005-0479-y>
- Betancur-R, R., Wiley, E. O., Arratia, G., Acero, A., Bailly, N., Miya, M., Lecointre, G., & Ortí, G. (2017). Phylogenetic classification of bony fishes. *BMC Evolutionary Biology*, 17(1), 162. <https://doi.org/10.1186/s12862-017-0958-3>
- Birdsong, R. S. (1975). The osteology of *Microgobius signatus* Poey (Pisces: Gobiidae), with comments on other gobioid fishes. *Bulletin of the Florida State Museum. Biological Sciences*, 19(3), 134–186.
- Birdsong, R. S., Murdy, E. O., & Pezold, F. L. (1988). A study of the vertebral column and median fin osteology in gobioid fishes with comments on gobioid relationships. *Bulletin of Marine Science*, 42(2), 174–214.
- Bleeker, P. (1849). Bijdrage tot de kennis der Blennioïden en Gobioiden van den Soenda-Molukschen Archipel, met beschrijving van 42 nieuwe soorten. *Verhandelingen van Het Bataviaasch Genootschap van Kunsten En Wetenschappen*, 22, 1–40.
- Bleeker, P. (1856). Beschrijvingen van nieuwe of weinig bekende vischsoorten van Manado en Makassar, grootendeels verzameld op eene reis naar den Molukschen Archipel in het gevolg van den Gouverneur Generaal Duymaer van Twist. *Acta Regiae Societatis Scientiarum et Litterarum Gothoburgensis. Zoologica*, 1(6), 1–80.

- Bradić-Milinović, K., Ahnelt, H., Rundić, L., & Schwarzahns, W. (2019).** The lost freshwater goby fish fauna (Teleostei, Gobiidae) from the early Miocene of Klinči (Serbia). *Swiss Journal of Palaeontology*, 138(2), 285–315. <https://doi.org/10.1007/s13358-019-00194-4>
- Brandl, S. J., Goatley, C. H. R., Bellwood, D. R., & Tornabene, L. (2018).** The hidden half: Ecology and evolution of cryptobenthic fishes on coral reefs. *Biological Reviews of the Cambridge Philosophical Society*, 93(4), 1846–1873. <https://doi.org/10.1111/brv.12423>
- Churchill, G. A., von Haeseler, A., & Navidi, W. C. (1992).** Sample size for a phylogenetic inference. *Molecular Biology and Evolution*, 9(4), 753–769.
- Cohen, K. M., Harper, D. A. T., & Gibbard, P. L. (2022).** *ICS International Chronostratigraphic Chart 2022/10*. International Commission on Stratigraphy, IUGS. Retrieved January 31, 2023, from <https://www.stratigraphy.org>
- Cuvier, G. (1816).** *Le règne animal distribué d'après son organisation: pour servir de base à l'histoire naturelle des animaux et d'introduction à l'anatomie comparée. Les reptiles, les poissons, les mollusques et les annélides* (Vol. 2). A. Belin.
- Edgar, R. C. (2004).** MUSCLE: Multiple sequence alignment with high accuracy and high throughput. *Nucleic Acids Research*, 32(5), 1792–1797. <https://doi.org/10.1093/nar/gkh340>
- Fabricius, J. C. (1779).** *Reise nach Norwegen mit Bemerkungen aus der Naturhistorie und Oekonomie*. Carl Ernest Bohn.
- Felsenstein, J. (1985).** Confidence limits on phylogenies: An approach using the bootstrap. *Evolution: International Journal of Organic Evolution*, 39(4), 783–791. <https://doi.org/10.2307/2408678>
- Fricke, R. (1983).** A method of counting caudal fin rays of actinopterygian fishes. *Braunschweiger Naturkundliche Schriften*, 1(4), 729–733.
- Fricke, R., Eschmeyer, W. N., & Fong, J. D. (2023).** *Eschmeyer's catalog of fishes: Genera/species by family/subfamily*. Retrieved January 17, 2023, from <https://research.calacademy.org/research/Ichthyology/catalog/SpeciesByFamily.asp>
- Froese, R., & Pauly, D. (2023).** *FishBase*. Retrieved December 2023, from <https://fishbase.org.au/v4>
- Gaudant, J. (1979).** Sur la présence de Gobiidae (Poissons téléostéens) dans l'Oligocène inférieur de Rouffach (Haut-Rhin). *Sciences Géologiques, Bulletin*, 32(3), 131–137. <https://doi.org/10.3406/sgeol.1979.1560>
- Gaudant, J. (1993).** L'ichthyofaune lacustre du Miocène d'Etili (Anatolie occidentale, Turquie): un réexamen. *Neues Jahrbuch für Geologie und Paläontologie – Monatshefte*, 1993(6), 335–344. <https://doi.org/10.1127/njgpm/1993/1993/335>
- Gaudant, J., & Quayle, W. J. (1988).** New palaeontological studies on the Chapelcorner fish bed (Upper Eocene, Isle of Wight). *Bulletin of the British Museum (Natural History) Geology*, 44(1), 15–39.
- Gelman, A., & Rubin, D. B. (1992).** Inference from iterative simulation using multiple sequences. *Statistical Science: A Review Journal of the Institute of Mathematical Statistics*, 7(4), 457–472. <https://doi.org/10.1214/ss/1177011136>
- Geyer, C. J. (1991).** Markov chain Monte Carlo maximum likelihood. In E. M. Keramidas (Ed.), *Computing science and statistics: Proceedings of the 23rd symposium on the Interface* (pp. 156–163). Interface Foundation.
- Gierl, C., Dohrmann, M., Keith, P., Humphreys, W., Esmaili, H. R., Vukić, J., Šanda, R., & Reichenbacher, B. (2022).** An integrative phylogenetic approach for inferring relationships of fossil gobioids (Teleostei: Gobiiformes). *PLoS One*, 17(7), e0271121. <https://doi.org/10.1371/journal.pone.0271121>
- Gierl, C., Liebl, D., Šanda, R., Vukic, J., Esmaili, H. R., & Reichenbacher, B. (2018).** What can goby otolith morphology tell us? *Cybium*, 42(4), 349–363.
- Gierl, C., & Reichenbacher, B. (2015).** A new fossil genus of Gobiiformes from the Miocene characterized by a mosaic set of characters. *Copeia*, 103(4), 792–805. <https://doi.org/10.1643/CI-14-146>
- Gierl, C., & Reichenbacher, B. (2017).** Revision of so-called *Pomatoschistus* (Gobiiformes, Teleostei) from the late Eocene and early Oligocene. *Palaeontologia Electronica*, 20.2.33A, 1–17. <https://doi.org/10.26879/721>
- Gierl, C., Reichenbacher, B., Gaudant, J., Erpenbeck, D., & Pharissat, A. (2013).** An extraordinary gobioid fish fossil from Southern France. *PLoS One*, 8(5), e64117. <https://doi.org/10.1371/journal.pone.0064117>
- Gill, A. C., & Mooi, R. D. (2012).** Thalasseleotrididae, new family of marine gobioid fishes from New Zealand and temperate Australia, with a revised definition of its sister taxon, the Gobiidae (Teleostei: Acanthomorpha). *Zootaxa*, 3266(1), 41–52. <https://doi.org/10.11646/zootaxa.3266.1.3>
- Gill, T. N. (1863).** Descriptions of the gobioid genera of the western coast of temperate North America. *Proceedings of the Academy of Natural Sciences of Philadelphia*, 15, 262–267.
- Goatley, C. H. R., & Tornabene, L. (2022).** *Tempestichthys bettyae*, a new genus and species of ocean sleeper (Gobiiformes, Thalasseleotrididae) from the central Coral Sea. *Systematics and Biodiversity*, 20(1), 1–15. <https://doi.org/10.1080/14772000.2022.2090633>
- Göktaş, F., & Ünay, E. (2000).** *The stratigraphy of the NW parts of the Akhisar (Manisa) Neogene basin*. International Earth Sciences Colloquium on the Aegean Region (IESCA-2000), İzmir.
- Goloboff, P. A. (1993).** Estimating character weights during tree search. *Cladistics: The International Journal of the Willi Hennig Society*, 9(1), 83–91. <https://doi.org/10.1111/j.1096-0031.1993.tb00209.x>
- Goloboff, P. A., & Catalano, S. A. (2016).** TNT version 1.5, including a full implementation of phylogenetic morphometrics. *Cladistics: The International Journal of the Willi Hennig Society*, 32(3), 221–238. <https://doi.org/10.1111/cla.12160>
- Goloboff, P. A., Torres, A., & Arias, J. S. (2018).** Weighted parsimony outperforms other methods of phylogenetic inference under models appropriate for morphology. *Cladistics: The International Journal of the Willi Hennig Society*, 34(4), 407–437. <https://doi.org/10.1111/cla.12205>
- Gosline, W. A. (1955).** The osteology and relationships of certain gobioid fishes, with particular reference to the genera *Kraemeria* and *Microdesmus*. *Pacific Science*, 9, 158–170.
- Gouy, M., Guindon, S., & Gascuel, O. (2010).** SeaView version 4: A multiplatform graphical user interface for sequence alignment and phylogenetic tree building. *Molecular Biology and Evolution*, 27(2), 221–224. <https://doi.org/10.1093/molbev/msp259>
- Guindon, S., Dufayard, J.-F., Lefort, V., Anisimova, M., Hordijk, W., & Gascuel, O. (2010).** New algorithms and

- methods to estimate maximum-likelihood phylogenies: Assessing the performance of PhyML 3.0. *Systematic Biology*, 59(3), 307–321. <https://doi.org/10.1093/sysbio/syq010>
- Günther, A. (1880).** *An introduction to the study of fishes*. A. and C. Black.
- Gut, C., Vukić, J., Šanda, R., Moritz, T., & Reichenbacher, B. (2020).** Identification of past and present gobies: Distinguishing *Gobius* and *Pomatoschistus* (Teleostei: Gobioidei) species using characters of otoliths, meristics and body morphometry. *Contributions to Zoology*, 89(3), 282–323. <https://doi.org/10.1163/18759866-bja10002>
- Harrison, I. J. (1989).** Specialization of the gobioid palatopterygoquadrate complex and its relevance to gobioid systematics. *Journal of Natural History*, 23(2), 325–353. <https://doi.org/10.1080/00222938900770211>
- Harrison, I. J. (1993).** The West African sicydiine fishes, with notes on the genus *Lentipes* (Teleostei: Gobiidae). *Ichthyological Exploration of Freshwaters*, 4(3), 201–232.
- Hasegawa, M., Kishino, H., & Yano, T. (1985).** Dating of the human-ape splitting by a molecular clock of mitochondrial DNA. *Journal of Molecular Evolution*, 22(2), 160–174. <https://doi.org/10.1007/BF02101694>
- Hilgen, F. J., Lourens, L. J., Van Dam, J. A., Beu, A. G., Boyes, A. F., Cooper, R. A., Krijgsman, W., Ogg, J. G., Piller, W. E., & Wilson, D. S. (2012).** Chapter 29 – The Neogene Period. In F. M. Gradstein, J. G. Ogg, M. D. Schmitz, & G. M. Ogg (Eds.), *The Geologic Time Scale* (pp. 923–978). Elsevier, Amsterdam.
- Hoese, D. F. (1984).** Gobioidei: Relationships. In H. G. Moser, W. J. Richards, D. M. Cohen, M. P. Fahay, A. W. Kendall Jr, & S. L. Richardson (Eds.), *Ontogeny and systematics of fishes* (pp. 588–591). The American Society of Ichthyologists and Herpetologists.
- Hoese, D. F., & Gill, A. C. (1993).** Phylogenetic relationships of eleotridid fishes (Perciformes: Gobioidei). *Bulletin of Marine Science*, 52(1), 415–440.
- Hoese, D. F., & Larson, H. K. (1987).** New Australian fishes. Part 11. A new genus and species of eleotridid (Gobioidea) from southern Australia with a discussion of relationships. *Memoirs of Museum Victoria*, 48(1), 43–50. <https://doi.org/10.24199/j.mmv.1987.48.11>
- Hoese, D. F., & Roberts, C. D. (2005).** A new species of the eleotrid genus *Thalasseleotris* (Teleostei: Gobioidei) from New Zealand coastal waters. *Journal of the Royal Society of New Zealand*, 35(4), 417–431. <https://doi.org/10.1080/03014223.2005.9517793>
- Höhna, S., Stadler, T., Ronquist, F., & Britton, T. (2011).** Inferring speciation and extinction rates under different sampling schemes. *Molecular Biology and Evolution*, 28(9), 2577–2589. <https://doi.org/10.1093/molbev/msr095>
- Iljin, B. S. (1930).** Le système des Gobiidés. *Trabajos Del Instituto Espanol de Oceanografia*, 2, 1–63.
- Jeon H.-B., Jun J., Choi S.-H., & Suk H. Y. (2021).** Diversification and colonization processes in Gobioidei predicted based on mitochondrial 12S rRNA with focusing on Oxudercidae. *Mitochondrial DNA. Part B, Resources*, 6(3), 1166–1172. <https://doi.org/10.1080/23802359.2021.1901620>
- Johnson, G. D., & Patterson, C. (1993).** Percomorph phylogeny: A survey of acanthomorphs and a new proposal. *Bulletin of Marine Science*, 52(1), 554–626.
- Kaya, O. (1981).** Miocene reference section for the coastal parts of West Anatolia. *Newsletter on Stratigraphy*, 10(3), 164–191. <https://doi.org/10.1127/nos/10/1981/164>
- Kaya, O., Ünay, E., Göktaş, F., & Saraç, G. (2007).** Early Miocene stratigraphy of central west Anatolia, Turkey: Implications for the tectonic evolution of the eastern Aegean area. *Geological Journal*, 42(1), 85–109. <https://doi.org/10.1002/gj.1071>
- Koken, E. (1891).** Neue Untersuchungen an tertiären Fisch-Otolithen II. *Zeitschrift Der Deutschen Geologischen Gesellschaft*, 43, 77–170.
- Lakner, C., van der Mark, P., Huelsenbeck, J. P., Larget, B., & Ronquist, F. (2008).** Efficiency of Markov chain Monte Carlo tree proposals in Bayesian phylogenetics. *Systematic Biology*, 57(1), 86–103. <https://doi.org/10.1080/10635150801886156>
- Lanfear, R., Calcott, B., Ho, S. Y. W., & Guindon, S. (2012).** Partitionfinder: Combined selection of partitioning schemes and substitution models for phylogenetic analyses. *Molecular Biology and Evolution*, 29(6), 1695–1701. <https://doi.org/10.1093/molbev/mss020>
- Lanfear, R., Frandsen, P. B., Wright, A. M., Senfeld, T., & Calcott, B. (2017).** PartitionFinder 2: New methods for selecting partitioned models of evolution for molecular and morphological phylogenetic analyses. *Molecular Biology and Evolution*, 34(3), 772–773. <https://doi.org/10.1093/molbev/msw260>
- Larsson, A. (2014).** AliView: A fast and lightweight alignment viewer and editor for large datasets. *Bioinformatics*, 30(22), 3276–3278. <https://doi.org/10.1093/bioinformatics/btu531>
- Lepage, T., Bryant, D., Philippe, H., & Lartillot, N. (2007).** A general comparison of relaxed molecular clock models. *Molecular Biology and Evolution*, 24(12), 2669–2680. <https://doi.org/10.1093/molbev/msm193>
- Lewis, P. O. (2001).** A likelihood approach to estimating phylogeny from discrete morphological character data. *Systematic Biology*, 50(6), 913–925. <https://doi.org/10.1080/106351501753462876>
- Lin, C.-H., Brzobohatý, R., Nolf, D., & Girone, A. (2017).** Tortonian teleost otoliths from northern Italy: Taxonomic synthesis and stratigraphic significance. *European Journal of Taxonomy*, 322, 1–44. <https://doi.org/10.5852/ejt.2017.322>
- Linnaeus, C. (1758).** *Systema naturae Regnum animale*. Guilielmi Engelmann.
- López-Antoñanzas, R., Mitchell, J. S., Simões, T. R., Condamine, F. L., Aguilée, R., Peláez-Campomanes, P., Renaud, S., Rolland, J., & Donoghue, P. C. J. (2022).** Integrative phylogenetics: Tools for palaeontologists to explore the Tree of Life. *Biology*, 11(8), 1185. <https://doi.org/10.3390/biology11081185>
- Maddison, W. P., & Maddison, D. R. (2021).** *Mesquite: A modular system for evolutionary analysis* (3.70) [Computer software]. <http://www.mesquiteproject.org>
- Marramà, G., Giusberti, L., & Carnevale, G. (2022).** A Rupelian coral reef fish assemblage from the Venetian Southern Alps (Berici Hills, NE Italy). *Rivista Italiana Di Paleontologia e Stratigrafia*, 128(2), 469–513. <https://doi.org/10.54103/2039-4942/16601>
- Martini, E., & Reichenbacher, B. (2007).** Nannoplankton und Fisch-Otolithen in den Mittleren Pechelbronnschichten (Unter-Oligozän, Oberrheingraben/Mainzer Becken) [Nannoplankton and fish otoliths from the Middle

- Pechelbronn Beds (Early Oligocene, Upper Rhine Graben/Mainz Basin)]. *Geologische Abhandlungen Hessen*, 116, 235–273.
- McCraney, W. T., Thacker, C. E., & Alfaro, M. E. (2020).** Supermatrix phylogeny resolves goby lineages and reveals unstable root of Gobiaria. *Molecular Phylogenetics and Evolution*, 151, 106862. <https://doi.org/10.1016/j.ympev.2020.106862>
- McKay, S. L., & Miller, P. J. (1997).** The affinities of European sand gobies (Teleostei: Gobiidae). *Journal of Natural History*, 31(10), 1457–1482. <https://doi.org/10.1080/00222939700770791>
- Miller, M. A., Pfeiffer, W., & Schwartz, T. (2010).** Creating the CIPRES Science Gateway for inference of large phylogenetic trees. *Proceedings of the Gateway Computing Environments Workshop (GCE)*, 1, 1–8.
- Miller, P. J. (1973).** The osteology and adaptive features of *Rhyacichthys aspro* (Teleostei: Gobioidi) and the classification of gobioid fishes. *Journal of Zoology*, 171(3), 397–434. <https://doi.org/10.1111/j.1469-7998.1973.tb05347.x>
- Miller, P. J. (1986).** Gobiidae. In P. J. P. Whitehead, M.-L. Bauchot, J.-C. Hureau, J. Nielsen, & E. Tortonese (Eds.), *Fishes of the north-eastern Atlantic and the Mediterranean* (Vol. 3, pp. 1019–1085). UNESCO.
- Nelson, J. S., Grande, T. C., & Wilson, M. V. H. (Eds.). (2016).** *Fishes of the world* (5th ed.). John Wiley & Sons.
- Obrhelová, N. (1961).** Vergleichende Osteologie der tertiären Süßwasserfische Böhmens (Gobioidi). *Sborník Ústředního Ústavu Geologického, Oddíl Paleontologický*, 26, 103–192.
- O'Reilly, J. E., Dos Reis, M., & Donoghue, P. C. J. (2015).** Dating tips for divergence-time estimation. *Trends in Genetics*, 31(11), 637–650. <https://doi.org/10.1016/j.tig.2015.08.001>
- Pallas, P. S. (1770).** *Spicilegia zoologica: quibus novae imprimis et obscurae animalium species iconibus, descriptionibus atque commentariis illustrantur* (Vol. 1). Gottl. August. Lange, Berlin.
- Papazzoni, C. A., Carnevale, G., Fornaciari, E., Giuberti, L., & Trevisani, E. (2014).** 4. The Pesciara-Monte Postale Fossil-Lagerstätte: 1. Biostratigraphy, sedimentology and depositional model. *Rendiconti Della Società Paleontologica Italiana*, 4, 29–36.
- Patzner, R., Van Tassel, J. L., Kovacic, M., & Kapoor, B. G. (Eds.). (2011).** *The biology of gobies* (1st ed.). Science Publishers.
- Pezold, F. (2004).** Phylogenetic analysis of the genus *Gobionellus* (Teleostei: Gobiidae). *Copeia*, 2004(2), 260–280. <https://doi.org/10.1643/CI-02-218R3>
- Popov, S. V., Rögl, F., Rozanov, A. Y., Steininger, F. F., Shcherba, I. G., & Kovac, M. (Eds.). (2004).** *Lithological-Paleogeographic maps of Paratethys: 10 maps Late Eocene to Pliocene* (1st ed., Vol. 250). Schweizerbart Science Publishers.
- Příkryl, T. (2014).** A new species of the sleeper goby (Gobioidi, Eleotridae) from the České Středohoří Mountains (Czech Republic, Oligocene) and analysis of the validity of the family Pirskeniidae. *Paläontologische Zeitschrift*, 88(2), 187–196. <https://doi.org/10.1007/s12542-013-0188-y>
- Pyron, R. A. (2017).** Novel approaches for phylogenetic inference from morphological data and total-evidence dating in squamate reptiles (lizards, snakes, and amphisbaenians). *Systematic Biology*, 66(1), 38–56. <https://doi.org/10.1093/sysbio/syw068>
- Rambaut, A. (2018).** *FigTree. Tree figure drawing tool* (1.4.4) [Computer software]. <http://tree.bio.ed.ac.uk/software/figtree/>
- Rambaut, A., Drummond, A. J., Xie, D., Baele, G., & Suchard, M. A. (2018).** Posterior summarization in Bayesian phylogenetics using Tracer 1.7. *Systematic Biology*, 67(5), 901–904. <https://doi.org/10.1093/sysbio/syy032>
- Rasser, M. W., Spiske, M., Battenstein, M., Achim, L., Ambrosius, R., Hanewinkel, A., & Müller, J. (2023).** Neues von der Fossilagerstätte Öhninger Maar (Mittelmiozän, Hegau) [News from the fossilagerstaette Öhningen Maar (Middle Miocene, Hegau)]. *Jahresberichte und Mitteilungen des Oberrheinischen Geologischen Vereins*, 105, 285–302. <https://doi.org/10.1127/jmogv/105/0012>
- Regan, C. T. (1911).** The osteology and classification of the gobioid fishes. *Annals and Magazine of Natural History*, 8(48), 729–733. <https://doi.org/10.1080/00222931108693090>
- Reichenbacher, B., & Bannikov, A. F. (2022).** Diversity of gobioid fishes in the late middle Miocene of northern Moldova, Eastern Paratethys – Part I: An extinct clade of *Lesueurigobius* look-alikes. *PalZ*, 96(1), 67–112. <https://doi.org/10.1007/s12542-021-00573-8>
- Reichenbacher, B., & Bannikov, A. F. (2023).** Diversity of gobioid fishes in the late middle Miocene of northern Moldova, Eastern Paratethys – Part II: description of †*Moldavigobius helenae* gen. et sp. nov. *PalZ*, 97(2), 365–381. <https://doi.org/10.1007/s12542-022-00639-1>
- Reichenbacher, B., & Schwarz, J. (1997).** Charophyten und Otolithen aus den Cyrenen-Schichten des nördlichen Alpenvorlandes [Charophytes and otoliths from the Cyrena Beds of the northern Alpine foreland]. *Paläontologische Zeitschrift*, 71(3), 173–188. <https://doi.org/10.1007/BF02988486>
- Reichenbacher, B., Gregorová, R., Holcová, K., Šanda, R., Vukić, J., & Příkryl, T. (2018).** Discovery of the oldest *Gobius* (Teleostei, Gobiiformes) from a marine ecosystem of Early Miocene age. *Journal of Systematic Palaeontology*, 16(6), 493–513. <https://doi.org/10.1080/14772019.2017.1313323>
- Reichenbacher, B., Krijgsman, W., Lataster, Y., Pippèr, M., Van Baak, C. G. C., Chang, L., Kälin, D., Jost, J., Doppler, G., Jung, D., Prieto, J., Abdul Aziz, H., Böhme, M., Garnish, J., Kirscher, U., & Bachtadse, V. (2013).** A new magnetostratigraphic framework for the Lower Miocene (Burdigalian/Ottmangian, Karpatian) in the North Alpine Foreland Basin. *Swiss Journal of Geosciences*, 106(2), 309–334. <https://doi.org/10.1007/s00015-013-0142-8>
- Reichenbacher, B., Příkryl, T., Cerwenka, A. F., Keith, P., Gierl, C., & Dohrmann, M. (2020).** Freshwater gobies 30 million years ago: New insights into character evolution and phylogenetic relationships of †Pirskeniidae (Gobioidi, Teleostei). *PloS One*, 15(8), e0237366. <https://doi.org/10.1371/journal.pone.0237366>
- Reichenbacher, B., Vukić, J., Šanda, R., Schliewen, U. K., Esmaeili, H. R., & Kassar, A. (2023).** Skeletal traits and otoliths can unravel the relationships within European Gobiidae (*Gobius* lineage *sensu lato*). *Zoological Journal*

- of the Linnean Society, zlad058. <https://doi.org/10.1093/zoolinnean/zlad058>
- Revell, L. J. (2024). phytools 2.0: An updated R ecosystem for phylogenetic comparative methods (and other things). *PeerJ*, 12, e16505. <https://doi.org/10.7717/peerj.16505>
- Ronquist, F., Klopfstein, S., Vilhelmsen, L., Schulmeister, S., Murray, D. L., & Rasnitsyn, A. P. (2012). A total-evidence approach to dating with fossils, applied to the early radiation of the hymenoptera. *Systematic Biology*, 61(6), 973–999. <https://doi.org/10.1093/sysbio/sys058>
- Ronquist, F., Lartillot, N., & Phillips, M. J. (2016). Closing the gap between rocks and clocks using total-evidence dating. *Philosophical Transactions of the Royal Society of London. Series B, Biological Sciences*, 371(1699), 20150136. <https://doi.org/10.1098/rstb.2015.0136>
- Ronquist, F., Teslenko, M., van der Mark, P., Ayres, D. L., Darling, A., Höhna, S., Larget, B., Liu, L., Suchard, M. A., & Huelsenbeck, J. P. (2012). MrBayes 3.2: Efficient Bayesian phylogenetic inference and model choice across a large model space. *Systematic Biology*, 61(3), 539–542. <https://doi.org/10.1093/sysbio/sys029>
- Rückert-Ülkümen, N. (1960). Trakya ve Canakkale mtakaiannda bulunan Neojen Balikli formasyonlan haklanda. *Fen Fakültesi. Istanbul Üniversitesi, Istanbul*.
- Rückert-Ülkümen, N. (2000). Eine neue Fisch-Fauna aus dem Tertiär von Bergama (West-Türkei). *Mitteilungen der Bayerischen Staatssammlung für Paläontologie und Historische Geologie*, 40, 153–163.
- Rüppell, E. (1838). *Neue Wirbelthiere zu der Fauna von Abyssinien gehörig. Fische des Rothen Meeres*. S. Schmerber, Frankfurt.
- Sauvage, H. E. (1883). Notes sur les poissons fossiles. *Bulletin de La Societe Geologique de France*, 3(11), 475–503.
- Schneider, C. A., Rasband, W. S., & Eliceiri, K. W. (2012). NIH Image to ImageJ: 25 years of image analysis. *Nature Methods*, 9(7), 671–675. <https://doi.org/10.1038/nmeth.2089>
- Schwarzahns, W. (Ed.) (2019). *Reconstruction of the fossil marine bony fish fauna (Teleostei) from the Eocene to Pleistocene of New Zealand by means of otoliths: With studies of recent congrid, morid and trachinoid otoliths* (Vol. 46). Museo Civico di Storia Naturale di Milano, Milano.
- Schwarzahns, W., Agiadi, K., & Carnevale, G. (2020). Late Miocene–Early Pliocene evolution of Mediterranean gobies and their environmental and biogeographic significance. *Rivista Italiana di Paleontologia e Stratigrafia*, 126(3), 657–724.
- Schwarzahns, W., Ahnelt, H., Carnevale, G., Japundžić, S., Bradić, K., & Bratishko, A. (2017). Otoliths in situ from Sarmatian (Middle Miocene) fishes of the Paratethys. Part III: tales from the cradle of the Ponto-Caspian gobies. *Swiss Journal of Palaeontology*, 136(1), 45–92. <https://doi.org/10.1007/s13358-016-0120-7>
- Schwarzahns, W., Brzobohatý, R., & Radwanska, U. (2020). Goby otoliths from the Badenian (middle Miocene) of the Central Paratethys from the Czech Republic, Slovakia and Poland: A baseline for the evolution of the European Gobiidae (Gobiiformes; Teleostei). *Bollettino della Società Paleontologica Italiana*, 59(2), 125–173.
- Simões, T. R., Caldwell, M. W., Talanda, M., Bernardi, M., Palci, A., Vernygora, O., Bernardini, F., Mancini, L., & Nydam, R. L. (2018). The origin of squamates revealed by a Middle Triassic lizard from the Italian Alps. *Nature*, 557(7707), 706–709. <https://doi.org/10.1038/s41586-018-0093-3>
- Speijer, R. P., Pälke, H., Hollis, C. J., Hooker, J. J., & Ogg, J. G. (2020). Chapter 28 – The Paleogene period. In F. M. Gradstein, J. G. Ogg, M. D. Schmitz, & G. M. Ogg (Eds.), *Geologic time scale 2020* (pp. 1087–1140). Elsevier.
- Springer, V. G. (1983). *Tyson belos*, new genus and species of Western Pacific fish (Gobiidae, Xenisthminae): With discussions of gobioid osteology and classification. *Smithsonian Contributions to Zoology*, 390, 1–40. <https://doi.org/10.5479/si.00810282.390>
- Stadler, T. (2010). Sampling-through-time in birth-death trees. *Journal of Theoretical Biology*, 267(3), 396–404. <https://doi.org/10.1016/j.jtbi.2010.09.010>
- Steindachner, F. (1879). Ichthyologische Beiträge (VIII). *Sitzungsberichte Der Kaiserlichen Akademie der Wissenschaften. Mathematisch-Naturwissenschaftliche Classe*, 80, 119–191.
- Tavare, S. (1986). Some probabilistic and statistical problems in the analysis of DNA sequences. *Lectures on Mathematics in the Life Sciences*, 17, 57–86.
- Temminck, C. J., & Schlegel, H. (1845). Pisces. In P. F. von Siebold (Ed.), *Fauna japonica, sive, descriptio animalium, quae in itinere per Japoniam, jussu et auspiciis, superiorum, qui summum in India Batava imperium tenent, suscepto, annis 1823–1830* (pp. 113–172). Lugduni Batavorum, Apud Auctorem.
- Thacker, C. E. (2009). Phylogeny of Gobioidi and placement within Acanthomorpha, with a new classification and investigation of diversification and character evolution. *Copeia*, 2009(1), 93–104. <https://doi.org/10.1643/CI-08-004>
- Thacker, C. E. (2013). Phylogenetic placement of the European sand gobies in Gobiellidae and characterization of gobiellid lineages (Gobiiformes: Gobioidi). *Zootaxa*, 3619(3), 369–382. <https://doi.org/10.11646/zootaxa.3619.3.6>
- Thacker, C. E. (2014). Species and shape diversification are inversely correlated among gobies and cardinalfishes (Teleostei: Gobiiformes). *Organisms, Diversity & Evolution*, 14(4), 419–436. <https://doi.org/10.1007/s13127-014-0175-5>
- Thacker, C. E. (2015). Biogeography of goby lineages (Gobiiformes: Gobioidi): Origin, invasions and extinction throughout the Cenozoic. *Journal of Biogeography*, 42(9), 1615–1625. <https://doi.org/10.1111/jbi.12545>
- Thacker, C. E., & Hardman, M. A. (2005). Molecular phylogeny of basal gobioid fishes: Rhyacichthyidae, Odontobutidae, Xenisthmidae, Eleotridae (Teleostei: Perciformes: Gobioidi). *Molecular Phylogenetics and Evolution*, 37(3), 858–871. <https://doi.org/10.1016/j.ympev.2005.05.004>
- Thacker, C. E., McCraney, W. T., Harrington, R. C., Near, T. J., Shelley, J. J., Adams, M., Hammer, M. P., & Unmack, P. J. (2023). Diversification of the sleepers (Gobiiformes: Gobioidi: Eleotridae) and evolution of the root gobioid families. *Molecular Phylogenetics and Evolution*, 186, 107841. <https://doi.org/10.1016/j.ympev.2023.107841>
- Thacker, C. E., Satoh, T. P., Katayama, E., Harrington, R. C., Eytan, R. I., & Near, T. J. (2015). Molecular

- phylogeny of Percomorpha resolves *Trichonotus* as the sister lineage to Gobioidae (Teleostei: Gobiiformes) and confirms the polyphyly of Trachinoidei. *Molecular Phylogenetics and Evolution*, 93, 172–179. <https://doi.org/10.1016/j.ympev.2015.08.001>
- Tornabene, L., Chen, Y., & Pezold, F. (2013).** Gobies are deeply divided: Phylogenetic evidence from nuclear DNA (Teleostei: Gobioidae: Gobiidae). *Systematics and Biodiversity*, 11(3), 345–361. <https://doi.org/10.1080/14772000.2013.818589>
- Tougard, C., Folly, J., & Berrebi, P. (2014).** New light on the evolutionary history of the common goby (*Pomatoschistus microps*) with an emphasis on colonization processes in the Mediterranean Sea. *PLoS One*, 9(3), e91576. <https://doi.org/10.1371/journal.pone.0091576>
- Tougard, C., Vukić, J., Ahnelt, H., Buj, I., Kovčić, M., Moro, G. A., Tutman, P., & Šanda, R. (2021).** Quaternary climatic cycles promoted (re)colonization and diversification events in Adriatic sand gobies. *Journal of Zoological Systematics and Evolutionary Research*, 59(5), 1037–1052. <https://doi.org/10.1111/jzs.12468>
- Valenciennes, A. (1837).** *Histoire naturelle des poissons* (G. Cuvier & A. Valenciennes, Eds.; Vol. 12). F. G. Levrault.
- Whitley, G. P. (1945).** New sharks and fishes from western Australia. Pt. 2. *The Australian Zoologist*, 11(1), 1–42.
- Wiley, E. O., & Johnson, G. D. (2010).** A teleost classification based on monophyletic groups. In J. S. Nelson, H.-P. Schultze, & M. V. H. Wilson (Eds.), *Origin and phylogenetic interrelationships of teleosts* (pp. 123–182). Verlag Dr. Friedrich Pfeil.
- Winterbottom, R. (1993).** Search for the Gobioid sister group (Actinopterygii: Percomorpha). *Bulletin of Marine Science*, 52(1), 395–414.
- Yang, Z. (1993).** Maximum-likelihood estimation of phylogeny from DNA sequences when substitution rates differ over sites. *Molecular Biology and Evolution*, 10(6), 1396–1401.
- Zhang, C., Stadler, T., Klopstein, S., Heath, T. A., & Ronquist, F. (2016).** Total-evidence dating under the fossilized birth-death process. *Systematic Biology*, 65(2), 228–249. <https://doi.org/10.1093/sysbio/syv080>
- Zharkikh, A. (1994).** Estimation of evolutionary distances between nucleotide sequences. *Journal of Molecular Evolution*, 39(3), 315–329. <https://doi.org/10.1007/BF00160155>

Associate Editor: Erin Maxwell